

# Solidification of Fluids

## Lecture Notes

Colin Meyer

### Contents

<b>1</b>	<b>Lecture on 17 January 2013</b>	<b>2</b>
1.1	Heat Transfer . . . . .	2
1.1.1	Derivation of the Advection-Diffusion Equation . . . . .	2
<b>2</b>	<b>Lecture on 29 January 2013</b>	<b>3</b>
2.1	Conservation of Heat at an Evolving Phase Boundary . . . . .	3
2.1.1	1D Solidification From a Cooled Boundary . . . . .	4
<b>3</b>	<b>Lecture on 31 January 2013</b>	<b>6</b>
3.1	Approximate Solution for Large Stefan Numbers . . . . .	6
3.2	1D Solidification from a Supercooled Melt . . . . .	7
3.2.1	Attachment Kinetics . . . . .	8
3.2.2	1D Solidification with Attachment Kinetics . . . . .	9
<b>4</b>	<b>Lecture on 4 February 2013</b>	<b>10</b>
4.1	Gibbs-Thomson Effect . . . . .	10
4.2	Linear Stability Analysis . . . . .	11
<b>5</b>	<b>Lecture on 5 February 2013</b>	<b>13</b>
5.1	Linearized Perturbation Equations . . . . .	13
5.2	Nucleation . . . . .	14
<b>6</b>	<b>Lecture on 7 February 2013</b>	<b>15</b>
6.1	Two Component Systems . . . . .	15
6.1.1	Equilibrium Phase Diagram . . . . .	15
6.1.2	Two Component 1D Solidification . . . . .	16
<b>7</b>	<b>Lecture on 1 February 2013</b>	<b>18</b>
7.1	Two Component Systems <i>continued</i> . . . . .	18
7.2	Constitutional Supercooling . . . . .	20
<b>8</b>	<b>Lecture on 12 February 2013</b>	<b>21</b>
8.1	Binary Phase Diagrams . . . . .	21
<b>9</b>	<b>Lecture on 14 February 2013</b>	<b>22</b>
9.1	Linear Stability Analysis for Two Component Systems . . . . .	22
9.2	Morphological Instability . . . . .	23
<b>10</b>	<b>Lecture on 19 February 2013</b>	<b>26</b>
10.1	Morphological Instability <i>continued</i> . . . . .	26
<b>11</b>	<b>Lecture on 21 February 2013</b>	<b>27</b>
11.1	Mushy Layers . . . . .	27
11.1.1	Evolution of Solid Fraction . . . . .	28

<b>12 Lecture on 26 February 2013</b>	<b>28</b>
12.1 Interfacial Conditions . . . . .	28
12.1.1 Condition of Marginal Equilibrium . . . . .	29
12.2 Conservation of Solute . . . . .	29
12.3 Reduced Equations for a Mushy Layer . . . . .	30
<b>13 Lecture on 28 February 2013</b>	<b>31</b>
13.1 Flow Inside a Mushy Layer . . . . .	32
13.1.1 Near-Eutectic Approximation . . . . .	32
13.2 Onset of Convection in a Horizontal Mushy Layer . . . . .	33
<b>14 Lecture on 5 March 2013</b>	<b>33</b>
14.1 Onset of Convection in a Horizontal Mushy Layer <i>continued</i> . . . . .	33
14.1.1 Parcel Argument . . . . .	35
<b>15 Lecture on 7 March 2013</b>	<b>35</b>
15.1 Interfacial Premelting . . . . .	35
15.1.1 Van Der Waals Interactions . . . . .	35
15.2 Premelting . . . . .	36
15.3 Lateral Heave in a Capillary Tube . . . . .	37
<b>16 Lecture on 12 March 2013</b>	<b>37</b>
16.1 Lateral Heave in a Capillary Tube <i>continued</i> . . . . .	37
16.2 Particle Migration . . . . .	38
16.2.1 Lubrication Analysis . . . . .	38

## 1 Lecture on 17 January 2013

### 1.1 Heat Transfer

Changes of phase are accompanied by the generation or absorption of *heat*. We will be concerned with the heat transfer by conduction and convection at evolving phase boundaries. The primary equation is the Advection-Diffusion Equation, that is derived here.

#### 1.1.1 Derivation of the Advection-Diffusion Equation

We will start with a volume  $V$  with normal vector  $\underline{u}$ , boundary  $S$ , and fluid flow  $\underline{u}$ , that contains specific enthalpy  $H$ . Here *specific* means that the flow is per unit mass. For systems at constant pressure, enthalpy and heat are identical (by the first law of thermodynamics). The conservation of enthalpy (heat) gives

$$\frac{d}{dt} \int_V \rho H dV = - \int_S \rho H (\underline{u} \cdot \underline{n}) dS - \int_S \underline{q} \cdot \underline{n} dS,$$

where  $\underline{q}$  is the heat flux. By differentiation under the integral sign and the divergence theorem we have

$$\int_V \frac{\partial}{\partial t} (\rho H) dV = - \int_V (\nabla \cdot (\rho H \underline{u}) - \nabla \cdot \underline{q}) dV,$$

Because the control volume is arbitrary this expression gives

$$\frac{\partial}{\partial t} (\rho H) + \nabla \cdot (\rho H \underline{u}) + \nabla \cdot \underline{q} = 0. \quad (1)$$

By Fourier's law of heat conduction, the heat flux can be written as

$$\underline{q} = -k \nabla T, \quad (2)$$

with  $k$  being the thermal conductivity. After expanding out some derivatives, this allows us to write equation (1) in the form

$$\rho \frac{\partial H}{\partial t} + H \left( \frac{\partial \rho}{\partial t} + \nabla \cdot (\rho \underline{u}) \right) + \rho \underline{u} \cdot \nabla H = \nabla \cdot (k \nabla T).$$

The second term in this last expression is zero by mass conservation. Using the relationship

$$\left. \frac{\partial H}{\partial T} \right|_p = \mathcal{C}_p,$$

where the subscript  $p$  indicates constant pressure and  $\mathcal{C}_p$  is the specific heat capacity at constant pressure, we find that

$$\rho \mathcal{C}_p \frac{\partial T}{\partial t} + \rho \mathcal{C}_p \underline{u} \cdot \nabla T = \nabla \cdot (k \nabla T).$$

This can be written as

$$\rho \mathcal{C}_p \frac{DT}{Dt} = \nabla \cdot (k \nabla T). \quad (3)$$

For a spatially constant thermal conductivity and defining the thermal diffusivity as

$$\kappa = \frac{k}{\rho \mathcal{C}_p},$$

the general form of the advection-diffusion equation found in equation (3) can be written as

$$\frac{\partial T}{\partial t} + \underline{u} \cdot \nabla T = \kappa \nabla^2 T, \quad (4)$$

which is nice analytically.

## 2 Lecture on 29 January 2013

### 2.1 Conservation of Heat at an Evolving Phase Boundary

The process of solidification occurs by crystallization. Hence, the boundary between solid and liquid does not move as no molecules move, rather they latch onto a growing lattice. This distinction is nuanced but it is an important point in terms of mass conservation. For this reason, the phase boundary *evolves* rather than *moves*. Furthermore it is useful to change the frame of reference to one where the phase boundary is stationary.

In this frame of reference, liquid now moves toward the interface with speed  $V_n$ , which is the rate at which the interface advances. There is a normal vector  $\underline{n}$  to the interface. A key assumption to this problem is that the interface between the solid and the liquid is at the freezing temperature,  $T_M$ , where the  $M$  stands for ‘Melt.’ Drawing a “pillbox” around an arbitrary location on the interface (this is essentially a 1D problem) we can write the balance for the heat entering and exiting the control volume as

$$\rho H_\ell V_n - \underline{n} \cdot \underline{q}_\ell - \rho H_s V_n + \underline{n} \cdot \underline{q}_s = 0,$$

where the first two terms are for the liquid (denoted by  $\ell$ ) and the second two are for the solid (denoted by  $s$ ). Rearranging we find that

$$\rho (H_\ell - H_s) V_n = \underline{n} \cdot \underline{q}_\ell - \underline{n} \cdot \underline{q}_s. \quad (5)$$

The change in enthalpy from a liquid to a solid is defined as the *latent heat of fusion* through<sup>1</sup>

$$\mathcal{L} = H_\ell - H_s.$$

Along with Fourier’s law for heat conduction, equation (2), we can write equation (5) as

$$\boxed{\rho \mathcal{L} V_n = k_s \left. \frac{\partial T}{\partial n} \right|_s - k_\ell \left. \frac{\partial T}{\partial n} \right|_\ell}.$$

This is referred to as the **Stefan Condition**.

<sup>1</sup>though since  $H_\ell$  and  $H_s$  are specific enthalpies,  $\mathcal{L}$  is the latent heat of fusion per unit mass.

Here it is important to note that this analysis assumed that the density of the solid was the same as the density of the liquid. This is, of course, rarely the case. More frequently,  $\rho_\ell \neq \rho_s$ . Thus, there is an induced velocity normal to the interface in the liquid that is

$$\underline{u}_n = \left( \frac{\rho_\ell - \rho_s}{\rho_\ell} \right) V_n,$$

which can be found by mass conservation. For water freezing into ice,  $\rho_\ell > \rho_s$ . Therefore, the induced velocity is positive and pushes away from the interface. This makes sense physically because the ice is expanding. In the case of unequal densities, the Stefan condition is

$$\rho_s \mathcal{L} V_n = k_s \left. \frac{\partial T}{\partial n} \right|_s - k_\ell \left. \frac{\partial T}{\partial n} \right|_\ell, \quad (6)$$

which comes from heat conservation (see Example Sheet 1).

### 2.1.1 1D Solidification From a Cooled Boundary

The schematic in this case is similar to the previous. There is a solid vertical wall (along the  $z$  axis at  $x = 0$ ) at temperature  $T_b$  which is less than the equilibrium freezing temperature  $T_M$ . A solid section of thickness  $a(t)$  grows steadily away from the wall in the  $x$ -direction. There is heat conduction through the solid but the liquid is at a constant temperature  $T_M$ , the same freezing/melting temperature. The rate of solidification is assumed to be slow (this assumption will be verified) and the system is close to thermodynamic equilibrium. This means that the interface at  $x = a(t)$  also has temperature,  $T_M$ . The only heat transfer is through the solid and only occurs by conduction. Thus, by the simplified advection-diffusion equation written here as equation (4), we have

$$\frac{\partial T}{\partial t} = \kappa \frac{\partial^2 T}{\partial x^2}$$

The boundary conditions are

$$T = \begin{cases} T_b & \text{at } x = 0 \\ T_M & \text{at } x = a(t) \end{cases}.$$

This problem is not simple because it is a *Free Boundary Problem*. That is, the condition at  $x = a(t)$  is not fixed – it is evolving! The additional constraint is the Stefan condition:

$$\rho \mathcal{L} \dot{a} = k \left. \frac{\partial T}{\partial x} \right|_{a-},$$

where the minus on  $a$  indicates that it is approaching the interface from the solid rather than the liquid.

Solutions can be found using Laplace transforms, however the better method is to use a similarity solution. Starting with dimensional considerations we want to scale the dimensions in the problem with a characteristic length  $L$ , a characteristic time  $\tau$ , and a temperature difference  $\Delta T$ . There is no external imposed length or timescale but there is an external temperature difference  $\Delta T = T_b - T_M$ . Using the arbitrary scales  $\tau$  and  $L$  we find from the diffusion equation (no advection in this problem) that

$$\frac{\Delta T}{\tau} \sim \kappa \frac{\Delta T}{L^2}.$$

Thus,

$$\boxed{L \sim \sqrt{\kappa \tau}}.$$

The boundary conditions are no help but the Stefan condition gives

$$\rho \mathcal{L} \frac{L}{\tau} \sim k \frac{\Delta T}{L} \sim \rho \mathcal{C}_p \kappa \frac{\Delta T}{L}.$$

This yields

$$L^2 \sim \left( \frac{\mathcal{C}_p \Delta T}{4 \mathcal{L}} \right) \kappa \tau,$$

which implies that

$$L \sim \frac{1}{\mathcal{S}^{\frac{1}{2}} \sqrt{\kappa \tau}},$$

where  $\mathcal{S}$  is the Stefan number:

$$\mathcal{S} = \frac{\mathcal{L}}{c_p \Delta T}$$

These two scaling relationships (the boxed equations above) give the same result. Thus, the two scaling equations are not independent. Therefore, there is no externally imposed timescale and the only logical choice is the elapsed time,  $\tau = t$ , which means that the lengthscale is then  $L \sim \sqrt{\kappa t}$ . Now we can write

$$T - T_b = (T_M - T_b) f\left(\frac{x}{L}, \frac{t}{\tau}\right).$$

However, since  $\tau = t$ , the similarity function  $f$  is not dependent on time. We can now rewrite the above equation in terms of a new function  $\theta$  is only dependent on the similarity variable  $\eta$ , where

$$T - T_b = (T_M - T_b) \theta(\eta) \quad \text{with} \quad \eta = \frac{x}{2\sqrt{\kappa t}}$$

The thickness of the solid region also needs to be nondimensionalized, the best choice is

$$a(t) = 2\lambda\sqrt{\kappa t}, \tag{7}$$

where  $\lambda$  is a dimensionless constant. Inserting the temperature scaling into the diffusion equation we find that

$$\theta'' = -2\eta\theta'. \tag{8}$$

where the primes (dashes) indicate derivatives with respect to  $\eta$ . In proving this, following derivatives are important

$$\frac{\partial \eta}{\partial t} = \frac{-2\eta}{4t} \quad \text{and} \quad \frac{\partial^2 \theta}{\partial x^2} = \theta'' \left(\frac{\partial \eta}{\partial x}\right)^2 = \frac{\theta''}{4\kappa t}.$$

Writing setting  $\theta'$  in equation (8) equal to  $\varphi$  we find that

$$\varphi' = -2\eta\varphi.$$

This equation easily separates and inserting  $\theta'$  back in we find that

$$\theta' = Ae^{-\eta^2},$$

where  $A$  is some unknown constant. Integrating one more time we find that

$$\theta(\eta) = A \int_0^\eta e^{-\varsigma^2} d\varsigma + C.$$

This integral is a minor rearrangement away from the error function, which is defined as

$$\text{erf}(x) = \frac{2}{\sqrt{\pi}} \int_0^x e^{-t^2} dt.$$

Thus, rolling the constants out in front into a new constant  $B$  we have

$$\theta(\eta) = B \text{erf}(\eta) + C$$

The boundary conditions can be converted into the similarity space as

$$\theta = \begin{cases} 0 & \text{at } \eta = 0 \\ 1 & \text{at } \eta = \lambda \end{cases},$$

and the Stefan condition is

$$2\mathcal{S}\lambda = \theta' \quad \text{at } \eta = \lambda.$$

Since the error function is zero at zero, the first of the temperature boundary conditions gives  $C = 0$ . The second one gives

$$\theta(\lambda) = 1 = \text{Berf}(\lambda) \longrightarrow B = \frac{1}{\text{erf}(\lambda)}$$

Thus,

$$\theta(\eta) = \frac{\text{erf}(\eta)}{\text{erf}(\lambda)}.$$

Thus, the temperature field is

$$T = T_b + (T_M - T_b) \frac{\text{erf}\left(\frac{x}{2\sqrt{\kappa t}}\right)}{\text{erf}(\lambda)}$$

Applying the Stefan condition we find that

$$2\mathcal{S}\lambda = \frac{2}{\sqrt{\pi}} \frac{e^{-\lambda^2}}{\text{erf}(\lambda)}.$$

where, the factor of 2 over square root of  $\pi$  comes from the definition of the derivative of the error function. Rearranging we find the phenomenal result that

$$\boxed{\mathcal{S}^{-1} = \sqrt{\pi} \lambda e^{\lambda^2} \text{erf}(\lambda)}. \quad (9)$$

This transcendental equation has solutions for all  $\lambda$  and  $\mathcal{S}$ . There is not an asymptote and the growth is exponential for large  $\lambda$ .

Some notes about this solution are:

1. This analysis is based on *slow growth* but  $\dot{a} \sim t^{-\frac{1}{2}}$  as  $t \rightarrow 0^+$ . This assumption is invalid for early times.
2. This similarity solution is an attractor as  $t \rightarrow \infty$ .
3. The growth of the crystal is slower (and the value of  $\lambda$  is smaller) when  $\mathcal{S}$  is larger. The physical reason for this is that there is more latent heat to removed. That is: a large Stefan number indicates slow growth.
4. For water/ice we have  $\mathcal{L}/\mathcal{C}_p \approx 80^\circ\text{C}$  which means that  $\mathcal{S} \approx 80/\Delta T$ . Thus, for a temperature difference of  $5^\circ\text{C}$ , the Stefan number is approximately  $\mathcal{S} \approx 16$ , which is fairly large, as  $\mathcal{S}^{-1} \approx 0.0625$ .

### 3 Lecture on 31 January 2013

#### 3.1 Approximate Solution for Large Stefan Numbers

The quasi-stationary approximation for large  $\mathcal{S}$ , and  $\lambda$  is small when  $\mathcal{S}$  is large, and this means small growth rates (by the Stefan condition). Time can be rescaled by the advance of the boundary as  $t \rightarrow \mathcal{S}t$ . Thus, the time derivative in the diffusion equation is  $O(\mathcal{S}^{-1})$  from

$$\mathcal{S}^{-1} \frac{\partial T}{\partial t} = \kappa \frac{\partial^2 T}{\partial x^2}.$$

Therefore, the time derivative term can be neglected in the large Stefan number limit. This means that

$$\frac{\partial T}{\partial x} = \text{constant} \approx \frac{T_m - T_b}{a(t)}.$$

For slow growth there is time for the temperature profile in the solid to equilibrate to the steady state *linear* profile. The Stefan condition gives

$$\rho \mathcal{L} \dot{a} \simeq k \frac{T_m - T_b}{a(t)}.$$

From the definition of the Stefan number,  $\mathcal{S} = \mathcal{L}/\mathcal{C}_p(T_m - T_b)$ , can rewrite this last equation to find the time dependent interface  $x = a(t)$  as

$$a(t) \simeq \sqrt{\frac{2\kappa t}{\mathcal{S}}}.$$

From the dimensional analysis performed in §2.1.1, equation (7) gives

$$a(t) = 2\lambda\sqrt{\kappa t} \simeq \sqrt{\frac{2\kappa t}{\mathcal{S}}} \longleftrightarrow \lambda \sim \sqrt{\frac{1}{2\mathcal{S}}},$$

for large Stefan numbers. To find the large  $\mathcal{S}$  limit of equation (9), we know that  $\lambda$  will be very small and thus

$$\lambda \ll 1 \longrightarrow e^{\lambda^2} \sim 1 \quad \text{and} \quad \text{erf}(\lambda) \sim \frac{2}{\sqrt{\pi}}\lambda.$$

From these approximations we have

$$\mathcal{S}^{-1} = \sqrt{\pi}\lambda e^{\lambda^2} \text{erf}(\lambda) \sim 2\lambda^2 \longrightarrow \lambda \sim \sqrt{\frac{1}{2\mathcal{S}}},$$

which is the same result as above. In this analysis we found that the rate of advance decreased with time. In the bag experiment, the rate was constant in time, though the experimental set up was slightly different. This is what we consider next.

### 3.2 1D Solidification from a Supercooled Melt

In the bag experiment the liquid was *supercooled*, which means that the liquid was below its equilibrium freezing temperature. Thus, the problem we will examine is the growth of a planar crystal into a supercooled melt. The diagram in this case is largely the same: There is a symmetry axis along the  $z$  axis at  $x = 0$  and the entire solid is maintained at a temperature  $T_M$  which is the equilibrium freezing temperature. A solid section of thickness  $a(t)$  grows steadily away from the wall in the  $x$ -direction. In the liquid, the temperature drops slowly away from  $T_M$  at the interface to the supercooled temperature  $T_\infty$  which is less than the equilibrium melting/freezing temperature  $T_M$ . The rate of solidification is assumed to be slow (this assumption will be verified) and the system is close to thermodynamic equilibrium. This means that the interface at  $x = a(t)$  also has temperature,  $T_M$ . Following a similar procedure as above we find the similarity equation

$$\theta'' = -2\eta\theta' \tag{10}$$

subject to the boundary conditions

$$\theta = \begin{cases} 1 & \text{on } \eta = \lambda \\ 0 & \text{for } \eta \rightarrow \infty \end{cases}$$

and the Stefan condition

$$2\mathcal{S}\lambda = -\theta' \quad \text{at } \eta = \lambda.$$

This minus sign is important because now the temperature change is occurring inside the liquid rather than in the previous example where the temperature changed inside of the solid. Thus, by equation (6), there is a minus sign. Integrating equation (10) we find the same condition as before

$$\theta = A \text{erf}(\eta) + B.$$

Inserting the boundary conditions we find that

$$\begin{aligned} 1 &= A \text{erf}(\lambda) + B \\ 0 &= A + B \end{aligned}$$

Thus, we determine that  $A = -B = -\text{erfc}(\lambda)$ , where  $\text{erfc}(z)$  is the complimentary error function, defined as:  $\text{erfc}(z) = 1 - \text{erf}(z)$ . This solution yields

$$\theta = \frac{\text{erfc}(\eta)}{\text{erfc}(\lambda)},$$

and the temperature field

$$T = T_\infty + (T_M - T_\infty) \frac{\operatorname{erfc}\left(\frac{x}{2\sqrt{\kappa t}}\right)}{\operatorname{erfc}(\lambda)}.$$

Inserting the similarity function  $\theta$  into the Stefan condition we have

$$2\mathcal{S}\lambda = \frac{2}{\sqrt{\pi}} \frac{e^{-\lambda^2}}{\operatorname{erfc}(\lambda)}.$$

This can be rearranged into the form

$$\mathcal{S}^{-1} = \sqrt{\pi}\lambda e^{\lambda^2} \operatorname{erfc}(\lambda). \quad (11)$$

Some notes about this solution:

1. As  $\lambda \rightarrow \infty$ , the Stefan number approaches unity from the positive  $\lambda$  side,  $\mathcal{S} \rightarrow 1_+$ . This can be shown elegant using the large  $\lambda$  expression of equation (11). For very large vales, the complimentary error function can be written as

$$\operatorname{erfc}(\lambda) \sim 1 - \left(1 - \frac{2}{\sqrt{\pi}} \int_\lambda^\infty e^{-\zeta^2} d\zeta\right) \sim \frac{2}{\sqrt{\pi}} \int_\lambda^\infty e^{-\zeta^2} d\zeta.$$

Thus, from (Hinch, 1991) we can integrate by parts to find that to first order

$$\operatorname{erfc}(\lambda) \sim \frac{2}{\sqrt{\pi}} \int_\lambda^\infty e^{-\zeta^2} d\zeta \sim \frac{e^{-\lambda^2}}{\lambda\sqrt{\pi}}$$

Inserting this large  $\lambda$  approximation into equation (11) we have that

$$\mathcal{S}^{-1} \sim \sqrt{\pi}\lambda e^{\lambda^2} \left(\frac{e^{-\lambda^2}}{\lambda\sqrt{\pi}}\right) \sim 1.$$

From a plot of of the transcendental equation found in equation (11), there is an asymptote to  $\mathcal{S} = 1$ .

2. What happens when  $\mathcal{S} < 1$ ? The transcendental equation found in equation (11) has no solution. This is different than the previous derivation in §2.1.1 because in the previous case there were solutions for all Stefan numbers, but in this case there is no solution for  $\mathcal{S} < 1$ . This means that there is *no similarity solution* for  $\mathcal{S} < 1$ .
3. The PDE develops singularities in finite time for  $\mathcal{S} \leq 1$ .

This singularity highlights a fault in the model. There is some addition physics that needs to be accounted for in the equations: the temperature is not exactly equal to  $T_M$  at the interface. The analysis above assumes that it is equal to  $T_M$ , but for  $\mathcal{S} \leq 1$ , this is no longer an appropriate assumption. This is rectified in the following sections.

### 3.2.1 Attachment Kinetics

Solidification is a reaction that depends on the level of disequilibrium driving it. At temperature  $T_M$  a solid-liquid interface is in dynamic equilibrium with molecules continually attaching and detaching at equal mean rates. The rates are described as *Arrhenius rates*. Although the mean rates are equal the absolute rates of attachment and detachment differ. Between 0 K (absolute zero) and  $T_M$  the rates are similar but the rate of attachment is slightly greater than the rate of detachment; the two rates are identical at 0 K and  $T_M$ . Above  $T_M$  the rate of detachment is increasingly greater than the rate of attachment. The rate of growth of the interface,  $V_n$ , is proportional to the difference between the attachment and detachment rates,  $R_A$  and  $R_D$  respectively, as  $V_n \propto (R_A - R_D)$ . Thus, when  $R_A > R_D$  the interface grows. A plot of the interfacial growth rate versus temperature shows that there is concave dependence, with a maximum around 100 K lower than  $T_M$ . The curve is negative for values larger than  $T_M$  and zero at 0 K and  $T_M$ . The is usually a large range of undercoolings, liquid that is below the freezing temperature, for which the interfacial velocity  $V_n$  is an increasing function of the temperature difference  $T_M - T_I$  where  $T_I$  is the unknown velocity of the interface.

For molecularly rough interfaces, where there is isotropic energy for crystallization i.e. no preferential direction of crystal growth, the growth rate of the interface is linear with respect to  $T_M - T_I$  and the constant of proportionality  $G$  is a constant material property. Thus,

$$V_n = G(T_M - T_I)$$



### 3.2.2 1D Solidification with Attachment Kinetics

Now the same problem as before, found in §3.2, can be solved, except that now the the interfacial temperature is an unknown  $T_I$  and the analysis includes attachment kinetics. Through this analysis it comes out that the interfacial growth rate is a constant in space and time, which is not utterly apparent from the set-up.

The equation is

$$\frac{\partial T}{\partial t} = \kappa \frac{\partial^2 T}{\partial x^2}$$

subject to the boundary conditions

$$T = \begin{cases} T_I & \text{at } x = a(t) \\ T_\infty & \text{at } x = \infty \end{cases}.$$

The Stefan condition gives

$$\rho \mathcal{L} \dot{a} = -k \left. \frac{\partial T}{\partial x} \right|_{a+},$$

and the linear material law (kinetic equation) is

$$\dot{a} = G(T_M - T_I).$$

The extra equation, material law, is needed in this case because the interfacial temperature  $T_I$  is an extra unknown. Scaling lengths with a lengthscale  $L$ , time with a timescale  $\tau$ , and temperature differences with  $\Delta T = T_M - T_\infty$ . The diffusion equation and the Stefan condition both give  $L \sim \sqrt{\kappa \tau}$  and the kinetic equation yields  $L \sim \tau G \Delta T$ . Equating these two we find that

$$L \sim \frac{\kappa}{G \Delta T},$$

$$\tau \sim \frac{\kappa}{G^2 \Delta T^2}.$$

These are different scalings than were found in the previous case. Nondimensionalizing the equations we find that

$$T = T_\infty + \Delta T \theta(x, t),$$

so that:

$$\frac{\partial \theta}{\partial t} = \frac{\partial^2 \theta}{\partial x^2},$$

subject to the boundary conditions

$$\theta = \begin{cases} \theta_I & \text{on } x = a(t) \\ 0 & \text{for } x \rightarrow \infty \end{cases}$$

and the Stefan condition

$$\mathcal{S} \dot{a} = - \left. \frac{\partial \theta}{\partial x} \right|_{a+},$$

and finally the kinetic equation gives

$$\dot{a} = 1 - \theta_I.$$

In general this couple set of partial differential equations does not have an analytic solution and certainly no similarity solution. For this reason we will examine the solutions for large and small Stefan numbers.

1. For  $\mathcal{S} \gg 1$ , from the Stefan condition we have that  $\dot{a} \sim O(\mathcal{S}^{-1})$ . Thus the kinematic equation yields

$$\theta_I \sim 1 + O(\mathcal{S}^{-1}).$$

This means that to leading order the temperature of the interface is the melting/freezing temperature, that is  $T_I = T_M$ , which is the assumption we made in the previous analysis in §3.2. In other words, for very large Stefan numbers we recover the similarity solution and there are no problems with asymptotes because the Stefan number is very much larger than unity. Furthermore, for  $\mathcal{S} > 1$ , it has been shown by Umantsev (1985) that the solutions to the full problem are asymptotic to the similarity solution as  $t \rightarrow \infty$ . The physical reason why the solution to the full problem approaches the similarity solution is that the rate of advance of the interface will slow down, justifying the assumptions made in the similarity analysis.

2. For  $\mathcal{S} \ll 1$ , we have a singular perturbation problem, because a  $\mathcal{S}$  becomes vanishingly small the order of the differential equation found in the Stefan condition is reduced. Thus, the Stefan condition is not a good evolution equation. The kinematic equation on the other hand does not have this problem and suggests looking for a solution of the form  $\dot{a} = V$ , where  $V$  is an unknown constant. Integrating we find that

$$a(t) = Vt$$

Next, we can use a moving origin, traveling wave solution

$$\theta = \theta(\eta) \quad \text{where} \quad \eta = x - Vt.$$

From the diffusion equation we have

$$-V\theta' = \theta'',$$

where the derivatives are with respect to  $\eta$ . This first order ODE has the solution

$$\theta = \theta_I e^{-V\eta}.$$

Plugging this into the Stefan condition we find that

$$\mathcal{S}V = V\theta_I \longrightarrow \theta_I = \mathcal{S},$$

and finally from the kinematic equation we have that

$$V = 1 - \mathcal{S}.$$

This gives a constantly advancing interface with temperature field

$$T = T_\infty + (T_M - T_\infty) \mathcal{S} e^{-(1-\mathcal{S})\eta}.$$

We also find that the interfacial temperature is a constant,  $\theta_I = \mathcal{S}$ , as postulated. This analysis is only physically valid for  $\mathcal{S} < 1$  because the the interface velocity  $V$  would be negative and the temperature field would increase exponentially. However, this solution is the long time attractor for all solutions to the full PDE, with Stefan numbers less than unity (Umantsev, 1985).

This analysis was excellent because it allowed to determine the long time behavior for the system for all values of  $\mathcal{S}$ . Although, there may be some initial unsteadiness, or dependence on initial conditions, all solutions tend towards the solutions described above, depending on their Stefan number. A natural question to ask is, how stable are these solutions? This will be explored in the next sections.

## 4 Lecture on 4 February 2013

### 4.1 Gibbs-Thomson Effect

A necessary tool to describe the stability of liquid-solid interfaces is the Gibbs-Thomson condition which describes the shape of an interface affects the physics: equilibrium freezing temperature is affected by curvature. The Clapeyron equation gives

$$\frac{\rho_s \mathcal{L} (T_M - T_e)}{T_M} = (p_s - p_\ell) + (p_\ell - p_M) \left( 1 - \frac{\rho_s}{\rho_\ell} \right),$$

where  $T_M$  is the equilibrium freezing/melting temperature at a reference pressure,  $p_M$ . The temperature  $T_e$  is the adjusted equilibrium temperature that takes pressure and density differences into account. As a quick aside, it is important to nondimensionalize temperature differences not absolute temperatures. For a planar melt, due to mechanical equilibrium, the liquid and solid pressures must be equal and thus,  $p_s = p_\ell$ .

For water, where  $\rho_s < \rho_\ell$  and if  $p_s = p_\ell > p_M$ , then the compensated temperature of equilibrium freezing/melting is lower, i.e.  $T_e < T_M$ . This is another way of saying: "Ice melts when you press on it!" This is incorrect reasoning as to why snowballs stick together. The general thought is that if you press the snow together into a ball it will melt slightly and then freeze back into shape. The amount of pressure you would need to exert is on the order of 100 atm. The same incorrect reasoning is applied to ice skating; the ice skates cannot exert 100 atmospheres of pressure on the ice.

For steel or another material where  $\rho_s > \rho_\ell$ , then when you exert pressure on the liquid, it becomes solid. This is the reason why the center of the earth, the hottest location and highest pressure, is solid.

Now considering the case where  $\rho_s = \rho_\ell$  (and  $p_s \neq p_\ell$ ) we have that

$$p_s - p_\ell = \gamma_{s\ell} \nabla \cdot \underline{n},$$

where  $\gamma_{s\ell}$  is the solid-liquid surface tension and  $\underline{n}$  is the unit normal point out of the solid and into the liquid. The term  $\nabla \cdot \underline{n}$  is the *curvature* and is referred to as  $K$ . The curvature of a sphere of radius  $R$  is  $2/R$ . Thus, the Clapeyron equation can be written as

$$\frac{\rho_s \mathcal{L} (T_M - T_e)}{T_M} = \gamma_{s\ell} \nabla \cdot \underline{n}.$$

With further rearranging we have

$$T_e = T_M - \Gamma \nabla \cdot \underline{n}.$$

The coefficient  $\Gamma$  is a collection of parameters defined as

$$\Gamma = \frac{\gamma_{s\ell} T_M}{\rho_s \mathcal{L}}.$$

In general the equilibrium freezing temperature can be dependent on the kinetics as well. Invoking the standard linear kinetic equation we have

$$V_n = G(T_e - T_I) = (T_M - \Gamma \nabla \cdot \underline{n} - T_I).$$

Now for a quick aside about equilibrium temperature. For a perfectly planar interface between liquid and solid the equilibrium freezing/melting temperature is  $T_M = 273.15$  K. There is no curvature of a perfectly straight, planar interface and therefore  $T_e = T_M$ . For a bath filled with ice cubes of varying size, the average  $T_e$  will be less than 273.15 K because of the curvature. If there is a large ice cube and a small ice cube the equilibrium freezing/melting temperature will be larger for the larger ice cube because it will have a smaller curvature. Imagine two spheres with  $R_1 > R_2$ , then,  $K_1 < K_2$ . Due to this temperature difference there will be a gradient between the two ice cubes and the larger ice cube will engulf the smaller one. This is called *Ostwald Ripening*.

Now for *Morphological Instabilities*: Imagine an curved interface between liquid and solid. Far from the interface the liquid is at temperature  $T_\infty$  and in the first case the interface is at temperature  $T_M$ , the melting/freezing temperature. At a point where the solid protrudes in the liquid the temperature isotherms are closer together as they bend around the protrusion, thus there is a larger heat flux. At a place where the liquid extends further into the solid, the isotherms are far apart and there is a very small heat flux. The combination means that protuberances tend to grow and valleys do not. However, if the interface is at a temperature  $T_e$ , which is greater than the melting/freezing temperature  $T_M$ , then the extent of the protuberances will be further than the  $T_M$  isotherm and tend to melt. The opposite is true for the valleys: the  $T_e$  isotherm will be inside of the  $T_M$  isotherm and tend to freeze. In this case, the Gibbs-Thomson effect is stabilizing. Armed with this analysis we can now do some linear stability analysis of a solid-liquid interface.

## 4.2 Linear Stability Analysis

The picture in this case is a two dimensional version of the single dimension crystal growth problems we have been examining. There is a finite width vertical channel, where one edge is the  $z$ -axis and at  $x = 0$ . The second edge is at some unspecified point in space and the  $y$  coordinates are not included. At  $z = 0$  there is some disturbance about the  $x$ -axis that has the temperature  $T_e$ . The disturbance is of the form  $z = \eta(x, t)$ . At  $z = H$  there is a symmetry axis with the temperature  $T_H$ . The entire system is moving at a constant velocity  $V$ , the rate of crystal growth. Thus we can move into a moving frame, where the unperturbed interface is steady. In this frame the equations are: Advection-diffusion

$$\kappa \nabla^2 T = \frac{\partial T}{\partial t} - V \frac{\partial T}{\partial z},$$

the Stefan condition

$$\rho \mathcal{L} \left( V + \frac{\partial \eta}{\partial t} \right) = - k \underline{n} \cdot \nabla T|_\ell,$$

there is no kinetic undercooling but these equations are subject to the boundary conditions

$$T = \begin{cases} T_M - \Gamma \nabla \cdot \underline{n} & \text{on } z = \eta(x, t) \\ T_H & \text{at } z = H \end{cases}$$

Scaling lengths with the location  $H$ , which is an unknown because it is not an external lengthscale, time with  $\mathcal{S}H^2/\kappa$ , and time with  $\Delta T = T_M - T_H$  we have

$$T = T_H + (T_M - T_H) \theta(x, z, t).$$

Thus, the equations can be written as

$$\nabla^2 \theta = \frac{1}{\mathcal{S}} \frac{\partial \theta}{\partial t} - Pe \frac{\partial \theta}{\partial z},$$

$$\theta = \begin{cases} \mathcal{S}Pe + \frac{\partial \eta}{\partial t} = -\underline{n} \cdot \nabla \theta & \text{for } z = \eta(x, t) \\ 1 - \frac{\gamma \nabla \cdot \underline{n}}{T_H} & \text{on } z = \eta(x, t) \\ T_H & \text{at } z = H \end{cases},$$

where  $Pe$  is the Péclet number, defined in this case as  $VH/\kappa$ . The lowercase  $\gamma$  is another collection of terms:  $\gamma = \Gamma/H\Delta T$ . This is distinct from the surface tension between liquid and solid  $\gamma_{sl}$ . For a surface  $g(x, z, t) = z - \eta(x, t)$  we can find the normal as

$$\underline{n} = \frac{\nabla g}{\|\nabla g\|} = -\frac{\left(\frac{\partial \eta}{\partial x}, 1\right)}{\sqrt{1 + \left(\frac{\partial \eta}{\partial x}\right)^2}} \approx -\left(\frac{\partial \eta}{\partial x}, 1\right).$$

The curvature  $K$  can be determined as

$$K = \nabla \cdot \underline{n} = \frac{-\frac{\partial^2 \eta}{\partial x^2}}{\left(1 + \left(\frac{\partial \eta}{\partial x}\right)^2\right)^{\frac{3}{2}}} \approx -\frac{\partial^2 \eta}{\partial x^2} \text{ for } \frac{\partial \eta}{\partial x} \ll 1.$$

Thus,

$$\boxed{\nabla \cdot \underline{n} \simeq -\frac{\partial^2 \eta}{\partial x^2}.$$

Taking a steady state base case  $\theta_0$  of the perturbation equations with  $\eta = 0$  we have that

$$\frac{\partial^2 \theta_0}{\partial z^2} = -Pe \frac{\partial \theta_0}{\partial z},$$

subject to

$$\theta_0 = \begin{cases} 1 & \text{at } z = 0 \\ 0 & \text{at } z = 1 \end{cases}$$

The solution to this differential equation is

$$\theta_0(z) = 1 - \frac{1 - e^{-Pe z}}{1 - e^{-Pe}}.$$

Inserting this into the Stefan condition we find

$$\mathcal{S} = \frac{1}{1 - e^{-Pe}} \longrightarrow \boxed{Pe = \ln \left( \frac{\mathcal{S}}{\mathcal{S} - 1} \right)}.$$

A few comments about this expression: first off, for a fixed rate of growth  $V$  and Stefan number  $\mathcal{S}$ , this relationship gives the height,  $H$ . Secondly, this expression only works if  $\mathcal{S} > 0$ . In the limit of very large Stefan number,  $\mathcal{S} \gg 1$ , this expression gives  $Pe \approx \mathcal{S}^{-1} \ll 1$ . Furthermore,

$$\boxed{\theta_0(z) \approx 1 - z.}$$

It is very common in large Stefan number limits to find a linear profile.

## 5 Lecture on 5 February 2013

### 5.1 Linearized Perturbation Equations

Starting off where we left off above, the perturbative effects can be added to the base case as

$$\theta = \theta_0(z) + \hat{\theta}(z)e^{i\alpha x + \sigma z},$$

$$\eta = 0 + \hat{\eta}e^{i\alpha x + \sigma t}.$$

Here  $\hat{\eta}$  is a constant number. The first perturbation equation is

$$\hat{\theta}'' - \alpha^2 \hat{\theta} = 0. \quad (12)$$

A Taylor expansion of the Stefan condition yields

$$\sigma \hat{\eta} = -\hat{\theta}' \quad \text{at } z = 0. \quad (13)$$

The term  $\mathcal{S}Pe$  is included in the base case and the  $\hat{\eta}\theta_0''$  term is zero because the base case is linear, for large  $\mathcal{S}$ . The modified Clapeyron equation can also be Taylor expanded to give

$$\hat{\theta} + \hat{\eta}\theta_0' = -\gamma\alpha^2 \hat{\eta} \quad \text{at } z = 0, \quad (14)$$

and finally the boundary condition is

$$\hat{\theta} = 0 \quad \text{at } z = 1.$$

Solving the first perturbation expression, modified advection-diffusion, found in equation (12) and applying the boundary conditions we have

$$\hat{\theta} = A \sinh(\alpha(1-z)).$$

In general, for finite domains it is convenient to use hyperbolic trigonometric functions and for infinite domains to use exponentials. This equation can then be inserted into equation (13) to find that

$$\sigma \hat{\eta} = A\alpha \cosh(\alpha).$$

Plugging in the hyperbolic expression into the modified Clapeyron equation (above equation (14)) we find that

$$A \sinh(\alpha) - \hat{\eta} = -\gamma\alpha^2 \hat{\eta},$$

where we have used the fact that  $\theta_0' = 0$ . Thus, using the last two equations, we can relate the stability parameter  $\sigma$  to the wavenumber  $\alpha$  through a dispersion relation:

$$\boxed{\sigma = \alpha(1 - \gamma\alpha^2) \coth(\alpha).}$$

The limits of this equation are:

1. For  $\alpha \ll 1$ ,  $\coth(\alpha) \rightarrow \frac{1}{\alpha} + \frac{\alpha}{3}$ . Thus,

$$\sigma \approx 1 + \left(\frac{1}{3} - \gamma\right)\alpha^2.$$

2. For  $\alpha \gg 1$ ,  $\coth(\alpha) \rightarrow 1$ , and therefore

$$\sigma \approx \alpha(1 - \gamma\alpha^2).$$

Plotting all three dispersion relations on a graph (actual, small  $\alpha$  limit, and large  $\alpha$  limit) demonstrates that for small  $\gamma$  the large  $\alpha$  limit expression gives very accurate results. The only part that it does not incorporate is a slight increase right around  $\alpha \approx 0$ . How often is  $\gamma \ll 1$ ? Since  $\gamma$  was a collection of terms, it can be written as

$$\gamma = \frac{\Gamma}{H\Delta T} = \frac{L_C}{H},$$

where  $\Gamma$  is the parameter from the Clapeyron equation (see §4.1) and  $L_C$  is the *Capillary Length*, defined as

$$L_C = \frac{\gamma_{sl} T_M}{\rho \mathcal{L} \Delta T}.$$

For water/ice, the surface tension between phases,  $\gamma_{sl} = 3.3 \times 10^{-2} \text{ N m}^{-1}$ , the latent heat of fusion  $\mathcal{L} = 334 \times 10^3 \text{ J kg}^{-3}$ , and with a density difference of  $\Delta T = 1 \text{ K}$  we find that  $L_C \approx 3 \times 10^{-8} = 30 \text{ nm}$ . This is extremely small! The thickness of the layer  $H$  is a lab scale on the order of millimeters or centimeters. Therefore, the ratio  $\gamma$  is very small and the large  $\alpha$  approximation can be used well.

The most unstable wavenumber is the maximum of the dispersion relation. This can be found by setting the derivative of the large  $\alpha$  expression equal to zero as

$$\frac{\partial}{\partial \alpha} (\alpha - \gamma \alpha^3) = 0 \longrightarrow 1 - 3\gamma \alpha_{max}^2 = 0 \longrightarrow \alpha_{max} = \frac{1}{\sqrt{3\gamma}}.$$

Thus, the most unstable wavelength is

$$\lambda_{max} = \frac{2\pi H}{\alpha_{max}} = 2\pi H \sqrt{3\gamma} \propto \sqrt{L_C H}.$$

This quantity,  $\sqrt{L_C H}$ , that the most unstable wavelength is proportional to is the geometric mean of the capillary length and the diffusion length scale. For the bag experiment,  $H \approx 10 \text{ cm}$  and assuming that the solution was water and ice (i.e.  $L_C \approx 3 \times 10^{-8}$ ), then the most unstable wavelength is on the order of  $\lambda_{max} \simeq 0.05 \text{ mm}$ . As an aside the stabilizing of the protuberance effect and capillarity gives the geometric mean. This is what sets the scale for snowflakes.

## 5.2 Nucleation

Consider a spherical particle in an infinite melt at temperature  $T_\infty < T_M$ . Employing the quasi-steady approximation, which is valid for large  $\mathcal{S}$ , then we have

$$\nabla^2 T = 0,$$

subject to

$$T = \begin{cases} T_\infty & r \rightarrow \infty \\ T_e = T_M - \frac{2\gamma_{sl} T_M}{\rho \mathcal{L} a} & r = a \end{cases}.$$

The only symmetric solutions to Laplace's equation in spherical coordinates are

$$T = A + \frac{B}{r}.$$

Applying the two boundary conditions we have

$$T = T_\infty + \left[ (T_M - T_\infty) - \frac{2\gamma_{sl} T_M}{\rho \mathcal{L} a} \right] \frac{r}{a}.$$

Inserting this expression into the Stefan condition we find that

$$\rho \mathcal{L} \dot{a} = \frac{k}{a} \left[ (T_M - T_\infty) - \frac{2\gamma_{sl} T_M}{\rho \mathcal{L} a} \right]$$

The growth rate of the radius,  $\dot{a}$ , can either be positive or negative and the sign depends on whether  $a$  is greater than a critical radius. That is,

$$a \geq a_{crit} \longleftrightarrow \boxed{a \geq \frac{2\gamma_{sl} T_M}{\rho \mathcal{L} (T_M - T_\infty)}} \longleftrightarrow a \geq 2L_C,$$

and  $a_{crit}$  is the critical radius for homogeneous nucleation. At  $-1^\circ \text{C}$  the critical radius is large, on the order of several nanometers. Although in our previous calculation we remarked that  $L_C$  is minute, on the scale of water molecules, which are about 1 angstrom ( $\text{\AA}$ ), tens of molecules need to crystallize before the critical radius is reached. For this reason, crystals typically grow heterogeneously on a foreign substrate. A classic example is ice growing on a flat solid impurity. The ice grows in such a way so that the radius of curvature of the sphere that would pass through the surface is much larger than the critical radius.

We can compute the time evolution of the radius through the Stefan condition:

1. For  $a \gg a_{crit}$ , we have that

$$\rho \mathcal{L} \dot{a} \simeq k \frac{T_M - T_\infty}{a}.$$

We have already solved this differential equation and have shown that the solution is proportional to the square root of time as  $a \propto \sqrt{t}$ .

2. For  $a \ll a_{crit}$ , then

$$\rho \mathcal{L} \dot{a} \simeq -\frac{2k\gamma_{sl}T_M}{\rho \mathcal{L} a^2}.$$

This differential equation can be solved for the time evolution of the radius as

$$a \simeq \left( a_0^3 - \frac{6k\gamma_{sl}T_M}{\rho^2 \mathcal{L}^2} t \right)^{\frac{1}{3}}.$$

The radius decreases to zero in finite time:

$$t_0 = \frac{a_0^3 \rho^2 \mathcal{L}^2}{6k\gamma_{sl}T_M}.$$

## 6 Lecture on 7 February 2013

### 6.1 Two Component Systems

To finish off the bag experiment we now need to look at two component systems. In this class, these are called *Alloys*: a mixture of two or more components, that are miscible in the liquid phase but possibly not miscible in the solid phase. Some examples of these are

1. Metals: *Bronze* can be made out of Copper & Lead or Copper & Tin. *Brass* is formed from either Copper & Zinc or Copper & Tin. *Steel* is the mixture of Iron & Carbon.
2. Other common mixtures include: Water & Alcohol (i.e. Scotch), Water & Salt (as in the ocean), and geological minerals (which can contain up to 10 components).

It is important to note that molten Bronze can be formed at a lower temperature than either molten Copper or molten Lead. In other words, the mixture typically freezes at a lower temperature than either of its members. For instance salt melts at 801 °C but water and salt is a liquid mixture at room temperature. This is also the reason why salt is placed on the road: salt and water freeze at a lower temperature than pure water. Often, as in the case with salt and water, when it freezes a different composition is formed. Sea ice is almost entirely freshwater.

#### 6.1.1 Equilibrium Phase Diagram

To make the statement about sea ice more exact it is beneficial to examine a *binary phase diagram*, see figure 1. There are many lines and symbols plotted on figure 1 and all of them are explained in the legend from the original paper. A few important definitions and symbols are described here. The line between the liquid ( $L$ ) and the crystalline solid & liquid ( $L + CS$ ) is called the *liquidus* and is represented as  $T_L(C)$  (or equivalently  $C_L(T)$ ). It is often approximated as linear, which is plotted in figure 1(b). The line between the crystalline solid & liquid ( $L + CS$ ) and the crystalline solid ( $CS$ ) is called the *solidus* and also is often approximated as the line  $T_S(C)$  or  $C_S(T)$ . As is shown on the plot, the standard phase diagram is symmetric. The point at which the two liquidus lines meet, the point of symmetry, is called the *eutectic*.

The regions of the phase diagram tell us what phases we have present, that exist at equilibrium give a sample of bulk composition  $C$  and temperature  $T$ . Above the eutectic temperature the only solid phase are called *solid solutions* in which molecules of  $B$  fit into the lattice of  $A$ ; for this reason, the solid is often represented as  $CS(A + b)$  for one half of the phase diagram. In the example of salt and ice, the molecules of salt don't fit very well into the lattice of freshwater ice. This is the reason that when saltwater freezes, the ice that is formed is primarily freshwater ice. An example of *complete solidification*, where the molecules of  $B$  fit perfectly into the lattice  $A$  and vice versa, is Olivine:  $(\text{Mg,Fe})_2\text{SiO}_4$ . This means that there is no eutectic point and that the phase diagram is asymmetrical. Below the eutectic temperature, in a standard binary phase diagram such as figure 1, a *composite solid* forms in which the grains of  $CSA$  coexist in equilibrium with grains of  $CSB$ .

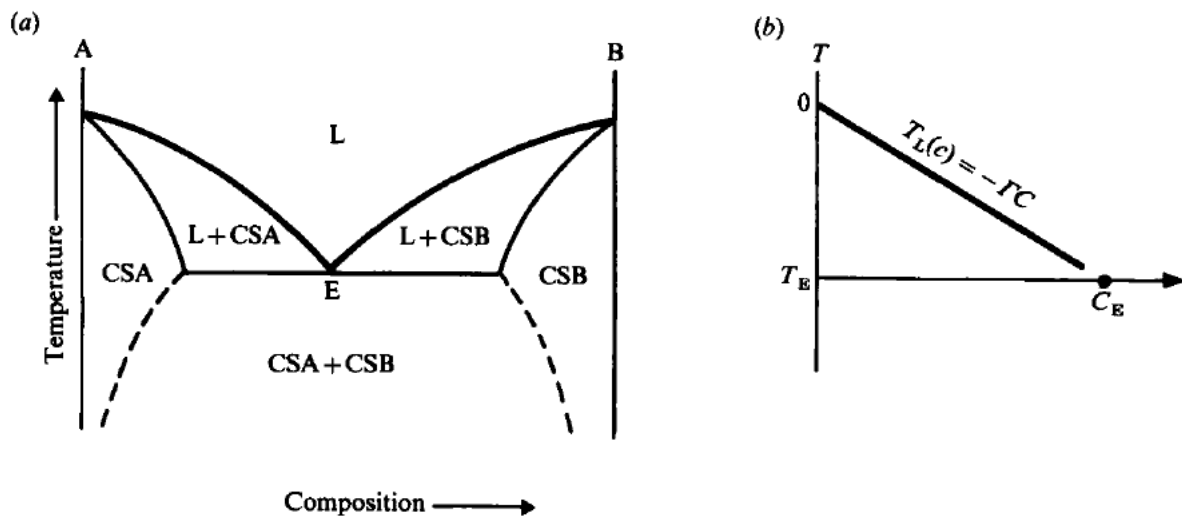


**FIGURE 1.** (a) Typical equilibrium phase diagram for a binary system comprising two components A and B. The liquidus —, the solidus —, and the dashed line ----, separate the diagram into regions of different phases: L, liquid; CSA, a crystalline solid in which molecules of B are incorporated into the crystal lattice of A; CSB, a crystalline solid in which molecules of A are incorporated into the crystal lattice of B; CSA + CSB, a granular solid in which crystalline grains of CSA are interspersed with grains of CSB. The solidus and the liquidus intersect at the eutectic point E. (b) The approximate phase diagram used in the mathematical analyses.

Figure 1: Binary phase diagram from Worster (1986)

For a given sample of bulk composition  $C_0$  and temperature  $T$  such that  $(C_0, T)$  lies between the solidus and liquidus, then in equilibrium there is a fraction  $\varphi$  of solid composition  $C_S(T)$  coexisting with liquid of composition  $C_L(T)$ . By the a conservation of solute we have

$$\varphi C_S + (1 - \varphi) C_L = C_0.$$

This relationship is called the *Lever Rule*. But in practice the fact that both the liquidus and solidus are approximated as linear functions, begets another relationship:

$$C_S(T) = k_D C_L(T),$$

where  $k_D$  is the constant distribution (or segregation) coefficient. This will often be assumed and sometimes  $k_D = 0$ .

### 6.1.2 Two Component 1D Solidification

Here we consider a similar problem to §2.1.1 except that there is diffusion in both phases and there is a concentration field. The solid evolves away from a solid boundary ( $x = 0$ ) that is held at a constant temperature  $T_B$ , which is less than  $T_M$ . The interface, at  $x = a(t)$ , has a constant temperature  $T_I$ . The far-field temperature in the liquid is  $T_\infty$ , which is greater than  $T_M$ . The concentration in the solid is a constant  $C_S$ ; this is under the assumption that the diffusivity in the solid,  $D_S = 0$ . Reasonable values suggest that  $D_S \approx 10^{-11} \text{ cm}^2 \text{ s}^{-1}$  and that the diffusivity in the liquid  $D \approx 10^{-5} \text{ cm}^2 \text{ s}^{-1}$ . Thus, diffusion is a million times ( $10^6$ ) greater in the liquid than in the solid and we can safely ignore it. There is a fairly dramatic jump in concentration at the interface up to the value  $C_I$ . This “pile-up” is due to the fact that the solid composition is often different than the liquid mixture; i.e. fewer molecules of B fit into the lattice of A. Presumably this would not occur for Olivine. The far-field concentration is  $C_0$ . An important connection between the temperature field and the concentration field occurs at the interface: under the assumption that the interface is in equilibrium we have

$$T_I = T_L(C_I) \quad \text{and} \quad C_S = k_D C_I.$$

As in the previous section,  $T_L(C_I)$  is the value on the liquidus line of the concentration  $C_I$  and the distribution coefficient  $k_D$  is used to connect the interface temperature from the liquidus line to the solidus.

From the above we can start by writing down the governing equations and the boundary conditions.



1. In the solid:

$$\frac{\partial T}{\partial t} = \kappa_s \frac{\partial^2 T}{\partial x^2}$$

$$T = \begin{cases} T_B, & x = 0 \\ T_I, & x = a(t) \end{cases}$$

2. In the liquid:

$$\frac{\partial T}{\partial t} = \kappa_l \frac{\partial^2 T}{\partial x^2},$$

$$\frac{\partial C}{\partial t} = D \frac{\partial^2 C}{\partial x^2},$$

$$T = \begin{cases} T_I, & x = a(t) \\ T_\infty, & x \rightarrow \infty \end{cases},$$

$$C = \begin{cases} C_I, & x = a(t) \\ C_0, & x \rightarrow \infty \end{cases}.$$

Both the solid and liquid phases are subject to the interfacial conditions. The Stefan condition is

$$\rho \mathcal{L} \dot{a} = k_s \left. \frac{\partial T}{\partial x} \right|_{x=a_-} - k_l \left. \frac{\partial T}{\partial x} \right|_{x=a_+}.$$

A similar condition exists in for the concentration field:

$$(C_I - C_S) \dot{a} = -D \left. \frac{\partial C}{\partial x} \right|_{x=a_+}.$$

As a aside the concentration condition can be derived from a conservation of solute argument. In other words the total area underneath the curve  $C(x, t)$  must stay the same. Thus,

$$\int_0^a (C_S - C_0) dx + \int_a^\infty (C - C_0) dx = 0. \quad (15)$$

Because this is a transient problem, we are interested in how the interface grows with time, we want the time derivative of equation (15). Since the thickness of the solid region  $a(t)$  is one of the limits of integration we must use the Leibniz integral rule which is

$$\frac{d}{dr} \left( \int_{n(r)}^{m(r)} f(p, r) dp \right) = \left( \int_{n(r)}^{m(r)} \frac{\partial f}{\partial r} dp \right) + f(m(r), r) \frac{\partial m}{\partial r} - f(n(r), r) \frac{\partial n}{\partial r}.$$

Writing equation (15) in this form we have

$$\int_0^a \frac{\partial}{\partial t} (C_S - C_0) dx + (C_S - C_0) \dot{a} + \int_a^\infty \frac{\partial}{\partial t} (C - C_0) dx - (C_I - C_0) \dot{a} = 0.$$

The first term is zero because  $C_S$  and  $C_0$  are constants, the second and fourth terms simplify, as does the integral in the third term. Hence we have

$$(C_S - C_I) \dot{a} + \int_a^\infty \frac{\partial C}{\partial t} dx = 0.$$

Inserting the time dependent diffusion relationship for the solute in the liquid phase and integrating once we have

$$(C_I - C_S) \dot{a} = D \left. \frac{\partial C}{\partial x} \right|_{x \rightarrow \infty} - D \left. \frac{\partial C}{\partial x} \right|_{x=a_+}.$$

The first term on the right side of this equation is zero because the concentration is equal to the constant  $C_0$  as  $x \rightarrow \infty$  and therefore there is no slope. Thus, we are left with the *concentration condition*:

$$\boxed{(C_I - C_S) \dot{a} = -D \left. \frac{\partial C}{\partial x} \right|_{x=a_+}.$$

## 7 Lecture on 1 February 2013

### 7.1 Two Component Systems *continued*

Simplifying the equations slightly we can set  $\kappa = \kappa_l = \kappa_s$ . There exists a similarity solution for this set of equations. We can write the thickness  $a(t)$  as

$$a(t) = 2\lambda\sqrt{Dt},$$

where the diffusivity of the solute,  $D$ , is used instead of the diffusivity of heat,  $\kappa$ . Thus, in the heat equations there is an extra factor of

$$\epsilon = \sqrt{\frac{D}{\kappa}}.$$

In this framework, the solutions will be exactly the same as before:

#### Solid

$$T = T_B + (T_I - T_B) \frac{\text{erf}(\epsilon\eta)}{\text{erf}(\epsilon\lambda)}$$

#### Liquid

$$T = T_\infty + (T_I - T_\infty) \frac{\text{erfc}(\epsilon\eta)}{\text{erfc}(\epsilon\lambda)}$$

$$C = C_0 + (C_I - C_0) \frac{\text{erfc}(\epsilon\eta)}{\text{erfc}(\epsilon\lambda)}$$

The interfacial conditions, the Stefan condition and the concentration condition give,

#### Stefan condition

$$\frac{\mathcal{L}}{\mathcal{C}_p} = \frac{T_I - T_B}{G(\epsilon\lambda)} - \frac{T_\infty - T_I}{F(\epsilon\lambda)}$$

#### Concentration condition

$$C_I - C_0 = \frac{C_I - C_0}{F(\lambda)}$$

where

$$F(z) = \sqrt{\pi}ze^{z^2}\text{erfc}(z)$$

$$G(z) = \sqrt{\pi}ze^{z^2}\text{erf}(z)$$

We will now examine the limit where

$$\epsilon = \sqrt{\frac{D}{\kappa}} \ll 1.$$

As the ratio of diffusivities of the solute and heat decreases, we find that

$$F(\epsilon) \sim \sqrt{\pi}\epsilon,$$

$$G(\epsilon) \sim 2\epsilon^2.$$

In the limit as  $\epsilon \rightarrow 0$ , the Stefan condition is

$$\frac{\mathcal{L}}{\mathcal{C}_p} = \frac{T_I - T_B}{G(\epsilon\lambda)} - \frac{T_\infty - T_I}{F(\epsilon\lambda)},$$

and the order of the terms is

$$O(1), O(\epsilon^{-2}), O(\epsilon^{-1}).$$

That is,

$$\frac{T_I - T_B}{G(\epsilon\lambda)} \sim O(\epsilon^{-2}).$$

Therefore, in this  $\epsilon \rightarrow 0$  limit, this term is much larger than all of the other terms and we have that

$$T_I = T_B + O(\epsilon), \quad \text{and} \quad C_I = C_B + O(\epsilon),$$

where  $T_B = T_L(C_B)$ . Thus, we can write the concentration condition as

$$C_I - C_S = \frac{C_I - C_0}{F(\lambda)} \rightarrow F(\lambda) \simeq \frac{C_B - C_0}{C_B - C_S} \equiv \mathcal{C}^{-1}.$$

Where the concentration ratio  $\mathcal{C}$  is defined as

$$\mathcal{C} = \frac{C_B - C_S}{C_B - C_0} = \frac{\text{Compositional difference across phase boundary}}{\text{Composition variation in the liquid}}.$$

This can be compared to the Stefan number

$$\mathcal{S} = \frac{\mathcal{L}}{C_p \Delta T} = \frac{H_B - H_S}{H_B - H_\infty} = \frac{\text{Enthalpy difference across phase boundary}}{\text{Scale for enthalpy variations in the liquid}}.$$

We can further compare  $F(\lambda) = \mathcal{C}^{-1}$  with  $F_{sc} = \mathcal{S}^{-1}$ , where  $F_{sc}(\lambda)$  is the equation from the solid growing in a supercooled melt (see equation (11) in §3.2). In the previous analysis, problems arose when  $\mathcal{S} < 1$ . However, the concentration ratio is always greater than unity,  $\mathcal{C} > 1$ . Thus, solutions to  $F(\lambda) = \mathcal{C}^{-1}$  always exist. There will be morphological instabilities however. It is important to note that a supercooled melt is metastable and can trigger instabilities. In a binary phase, the components are stable but instabilities develop.

As a final note on this solution, the thickness of solid,  $a = 2\lambda\sqrt{Dt}$  with  $\lambda = O(1)$ , slows as  $\epsilon \rightarrow 0$ . That is, the rate of solid growth is dictated by the diffusion of the solute. So, for a planar interface the diffusion of the solute is rate controlling as the solute must diffuse away from the interface before it can solidify. This is true unless  $C_0 - C_S = O(\epsilon)$ , i.e. when the melt is almost pure, then it will be thermally controlled.

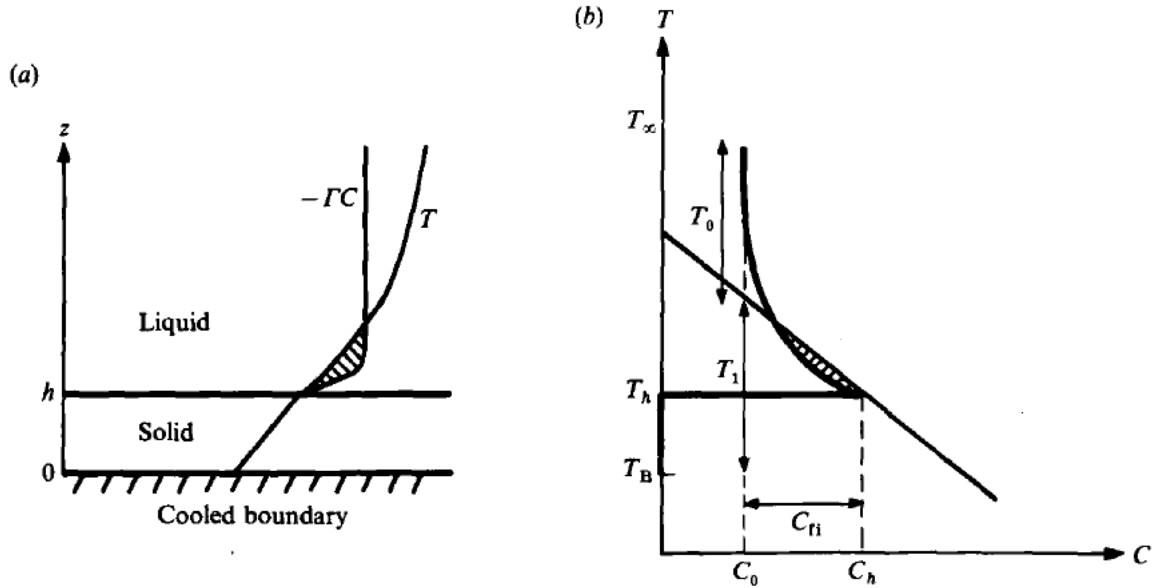


**FIGURE 2.** (a) Schematic diagram of solidification from a plane wall when the solid/liquid interface is flat. The hatched region shows where the liquid is supercooled – where the temperature  $T$  is below the local liquidus temperature  $-\Gamma C$ . (b) A schematic plot of  $(T(z), C(z))$  defining the variables used in the mathematical analyses.

Figure 2: Constitutional supercooling diagram from Worster (1986)

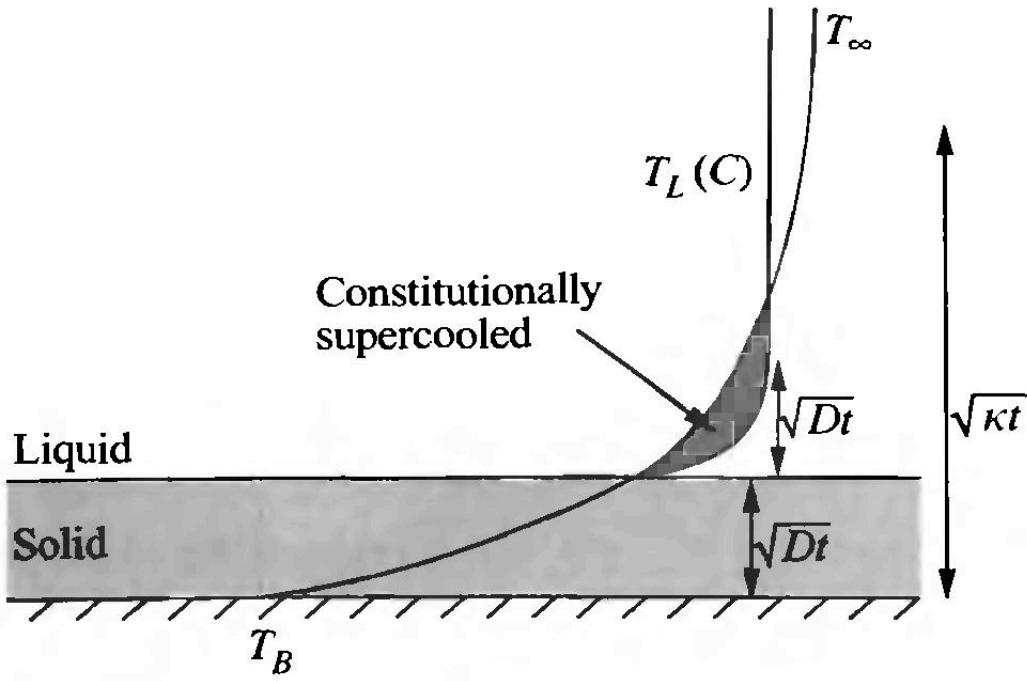


Figure 3: Diagram from Batchelor et al. (2000). This diagram shows the one-dimensional solidification of a binary alloy. The rate of solidification is limited by the rate of transport of the solute away from the the liquid-solid interface where it is rejected. The solute then accumulates in a compositional boundary layer causing a local depression in the freezing temperature. Since the heat diffuses much more rapidly than the solute ( $\kappa \ll D$ ), a region of constitutional supercooling results, as shown.

## 7.2 Constitutional Supercooling

It is convenient to plot the local freezing temperature field on the same diagram with the temperature curve; examples can be found in figures 2 and 3. The local liquidus temperature is  $T_L(C) = T_M - \Gamma C$ . In the shaded region the temperature of the liquid is below the local liquidus temperature (freezing temperature). This is known as *constitutional supercooling*. The reason for this is that the reject solute accumulates ahead of the interface and lowers the local freezing temperature. Furthermore, since the thermal boundary layer is much broader than the boundary layer of the solute, the temperature remains close to the interfacial temperature. Therefore, for much of the solute boundary layer, the fluid is supercooled. The condition for constitutional supercooling to is

$$\left. \frac{\partial T}{\partial x} \right|_{a_+} < \left. \frac{\partial T_L}{\partial x} \right|_{a_+}$$

Comparing these two quantities we have

$$\frac{\left. \frac{\partial T}{\partial x} \right|_{a_+}}{\left. \frac{\partial T_L}{\partial x} \right|_{a_+}} = \frac{\frac{\partial}{\partial \eta} \left( T_\infty + (T_I - T_\infty) \frac{\text{erfc}(\epsilon \eta)}{\text{erfc}(\epsilon \lambda)} \right) \Big|_\lambda}{\frac{\partial}{\partial \eta} \left( T_M - \Gamma \left( C_0 + (C_I - C_0) \frac{\text{erfc}(\eta)}{\text{erfc}(\lambda)} \right) \right) \Big|_\lambda} = \frac{(T_I - T_\infty) \frac{-2\epsilon e^{-\epsilon^2 \lambda^2}}{\sqrt{\pi} \text{erfc}(\epsilon \lambda)}}{-\Gamma (C_I - C_0) \frac{-2e^{-\lambda^2}}{\sqrt{\pi} \text{erfc}(\lambda)}} \cdot \frac{\epsilon}{\frac{1}{\lambda}} < 1.$$

Whence,

$$\frac{\left. \frac{\partial T}{\partial x} \right|_{a_+}}{\left. \frac{\partial T_L}{\partial x} \right|_{a_+}} = \frac{(T_\infty - T_I)}{\Gamma (C_I - C_0)} \frac{\epsilon^2 F(\lambda)}{F(\epsilon \lambda)} < 1.$$

where  $\Gamma$  is the slope:  $\Gamma = T'_L(C)$ . Constitutional supercooling occurs when this quantity is less than one. For small  $\epsilon$ , this quantity is  $O(\epsilon)$  because  $F(\epsilon \lambda) \sim O(\epsilon)$  as  $\epsilon \rightarrow 0$ . Therefore, constitutional supercooling frequently occurs. Three ways to avoid it are:

1. When the melt is almost pure, i.e.  $(C_I - C_0) \sim \epsilon$ , then the condition is order unity.

2. If the melt is cooled slowly or there is a small temperature difference, then constitutional supercooling can be avoided.
3. Lastly, if  $\epsilon$  is not vanishingly small. This can be achieved by imposing some flow with an eddy diffusivity of solute  $D_E$  in the liquid.

A graph of this inequality can be found in Huppert and Worster (1985) and shows the conditions under which constitutional supercooling will occur in the melt as a function of the initial solute concentration,  $C_0$ , and boundary temperature,  $T_B$ . The result of constitutional supercooling in a melt is the formation of a mushy region from the development of morphological instabilities.

## 8 Lecture on 12 February 2013

### 8.1 Binary Phase Diagrams

This lecture consisted of drawing binary phase diagrams for different initial conditions. In lieu of drawing all of them, I will describe them in words.

1. The first drawing is to change our standard picture only slightly by make a nonzero distribution coefficient,  $k_D \neq 0$ . This means that the solidus line is no longer vertical and that the solid is a compositional mixture. For sea ice, the solid phase is almost entirely pure water and therefore we can approximate that  $k_D = 0$ . However, other alloys behave differently (recall Olivine). Hence, the nonzero distribution coefficient case is important. Essentially, in this case, the the temperature—concentration profile starts in the liquid region and then dips below the liquidus, where they may be a region of constitutional supercooling. Then there is a jump in concentration over to the solidus and the profile is a vertical line in the solid region to the final temperature. This is assuming that there is no solute diffusion in the solid. It is also important to remember that the same processes can be seen on both sides of the eutectic.
2. The next drawing is to see what happens during the solidification of a eutectic melt. That is, starting at some large temperature in the liquid regime but with the eutectic composition, when it is cooled, the composition doesn't change. The physical reason for this is that there is a build up of solute at the interface and thus the temperature—concentration profile moves toward larger values of concentration. The same is true, however, from the opposite side, due to the symmetry of the Binary phase diagram. Thus, there are restoring actions to keep the eutectic concentration, in other words, this solidification occurs exactly as in a pure melt. Once the eutectic point ( $C_E, T_E$ ) has been reached the solidification continues but into a new regime. It is no longer the crystalline solid CS(A+b) but now a composite solid CS(A+b)+CS(B+a), see figure 1. This solidifying process is not rate limited by the diffusion of the solute.
3. Another important case is when the the temperature of the boundary is below the eutectic temperature and the starting temperature is in the liquid regime. This means that the temperature—concentration profile must pass through the eutectic point, in other words, the interfacial composition is the eutectic composition. The final composition is order  $\epsilon^2$  away from the initial composition. This can be seen from the fact that  $C_I = C_E$ ; solute conservation gives

$$(C_E - C_S) \dot{a} = -D \left. \frac{\partial C}{\partial x} \right|_{a+}$$

from  $a(t) = 2\lambda\sqrt{\kappa t}$  and

$$C = C_0 + (C_E - C_0) \frac{\text{erfc}(\epsilon\eta)}{\text{erfc}(\epsilon\lambda)}$$

4. Melting versus dissolving: melting is not the only way for components to change phase. A simple example is an ice cube in tin foil placed in the Arctic Ocean ( $-2^\circ\text{C}$ ) will not melt. However, if this same ice cube was placed in the Arctic Ocean (without the tin foil) it will *dissolve*.
5. Isothermal. In this case, the temperature in the liquid far away from the interface ( $T_\infty$ ) is the same as the temperature far away from the interface in the solid ( $T_{-\infty}$ ). That is,  $T_\infty = T_{-\infty}$ . At the interface, however, the temperature is lower because there is salt in the water.
6. Directional Solidification: For a constant casting rate, there cannot be a steady state if the distribution coefficient  $k_D = 0$  because salt is always being produced (an infinite amount).

## 9.1 Linear Stability Analysis for Two Component Systems

Starting with a directional solidification set-up similar to the previous work on linear stability analysis in §4.2. There are two sets of heat exchangers, one at  $z = z_H$  and one at  $z = z_C$  which maintain the temperatures at  $T_H$  and  $T_C$  respectively. The interface is at  $z = 0$ , such that  $z_H > 0 > z_C$ . The entire system is advecting down at a speed  $V$ .

In steady state, the concentration of solute in the solid is constant,  $C_s = C_0$ . Through the distribution coefficient we have that

$$C_0 = k_D C_I.$$

Therefore, once we know the solid composition we know the interfacial composition. The equations describing this system are

$$\begin{aligned} -V \frac{\partial T}{\partial z} &= \kappa \frac{\partial^2 T}{\partial z^2} \quad \text{in both phases.} \\ -V \frac{\partial C}{\partial z} &= D \frac{\partial^2 C}{\partial z^2} \end{aligned}$$

Starting with the temperature field and integrating once we find that

$$A_C - \frac{V}{\kappa} = \ln \left( \frac{\partial T}{\partial z} \right) \longrightarrow \frac{\partial T}{\partial z} = B_C e^{-\frac{V}{\kappa} z}.$$

Thus,

$$T = D_C + B_C e^{-\frac{V}{\kappa} z}.$$

Here  $A_C$ ,  $B_C$ , and  $D_C$  are arbitrary constants. Inserting the boundary conditions for the liquid we have

$$T(z = 0) = T_I \longrightarrow D_C + B_C = T_I,$$

$$T(z_H) = T_H \longrightarrow D_C = T_H,$$

under the approximation that  $z_H \gg V/\kappa$ . Thus, the temperature field in the liquid is

$$T = T_H + (T_I - T_H) e^{-\frac{V}{\kappa} z}.$$

Using the same solution to the differential equation we can insert the boundary conditions for the solid phase as

$$T(z_C) = T_C \longrightarrow D_C + B_C e^{-\frac{V}{\kappa} z_C} = T_C,$$

$$T(z = 0) = T_I \longrightarrow D_C + B_C = T_I.$$

Solving for  $D_C$  and  $B_C$  in terms of  $T_I$  and  $T_C$ , we find that

$$\begin{aligned} B_C &= \frac{T_I - T_C}{\left(1 - e^{-\frac{V}{\kappa} z_C}\right)}, \\ D_C &= T_C - \frac{(T_I - T_C) e^{-\frac{V}{\kappa} z_C}}{\left(1 - e^{-\frac{V}{\kappa} z_C}\right)}. \end{aligned}$$

Therefore, the temperature profile in the solid phase is

$$T = T_C - (T_I - T_C) \left( \frac{e^{-\frac{V}{\kappa} z} - e^{-\frac{V}{\kappa} z_C}}{1 - e^{-\frac{V}{\kappa} z_C}} \right).$$

Solving the same ODE for the concentration in the liquid we have that

$$C = D_C + B_C e^{-\frac{V}{D} z}.$$

The boundary conditions are

$$\begin{aligned} C(z_H) &= C_0 \longrightarrow D_C = C_0, \\ C(z=0) &= k_D C_0 \longrightarrow D_C + B_C = k_D C_0. \end{aligned}$$

If the approximation is used that  $z_H \gg D/V$  then

$$C = C_0 + \left( \frac{1 - k_D}{k_D} \right) C_0 e^{-\frac{V}{\kappa} z}.$$

Now we make the *Frozen Temperature Approximation* by assuming that

$$\frac{D}{V} \ll z_H \ll \frac{\kappa}{V}.$$

This is okay to do, in part, because  $D/\kappa \ll 1$ . This gives linear approximations of the temperature field in both the liquid and solid. There is a break in slope due to latent heat. We will also assume that

$$\frac{\mathcal{L}}{\mathcal{C}_p(T_H - T_C)} \frac{V(z_H - z_C)}{\kappa} \ll 1.$$

Which is another way of writing

$$\mathcal{S}Pe \ll 1,$$

where  $\mathcal{S}$  is the Stefan number and  $Pe$  is the Péclet number. This is a practical limit for slow evolution, i.e.,  $D/\kappa \ll 1$  and  $V \ll 1$ . The Stefan condition shows that the break in slope is asymptotically small and therefore we can assume one single temperature profile, given by

$$T = T_C + (T_H - T_C) \left( \frac{z - z_C}{z_H - z_C} \right).$$

This is linear and constant in time. The growth of linear perturbations is slow compared to the rate of heat transfer across the system. This profile can be simplified to

$$T = T_0 + Gz, \quad \text{where} \quad G = \frac{T_H - T_C}{z_H - z_C} = \text{constant}.$$

Here  $T_0$  is on the liquidus at the interfacial temperature, i.e.,

$$T_0 = T_L \left( \frac{C_0}{k_D} \right).$$

The phase diagram can be simplified to a linear *liquidus line* as

$$T_L = T_0 - m \left( C - \frac{C_0}{k_D} \right),$$

where  $m$  is the constant liquidus slope.

## 9.2 Morphological Instability

Now we examine the morphological instability under the frozen temperature approximation. The base case is what was just derived, now a sinusoidal perturbation can be added to the concentration field yielding the temperature and concentration equations as

$$T = T_0 + Gz,$$

$$C = C_0 + \left( \frac{1 - k_D}{k_D} \right) C_0 e^{-\frac{V}{\kappa} z} + \hat{\phi}(\zeta) e^{i\alpha\zeta + \sigma\tau}. \quad (16)$$

Where the  $\xi$ ,  $\tau$ , and  $\zeta$  are nondimensional variables, related to  $x$ ,  $t$ , and  $z$  through the interface advance speed  $V$  and the diffusivity of salt  $D$ , as

$$x = \frac{D}{V}\xi \quad \text{and} \quad z = \frac{D}{V}\zeta \quad \text{and} \quad t = \frac{D}{V^2}\tau.$$

The solid-liquid interface is moved to  $z = \eta$  which is also perturbed as

$$z = \eta = \hat{\eta}e^{i\alpha\xi + \sigma\tau}.$$

Here the concentration field satisfies the full advection-diffusion equation given by

$$\frac{\partial C}{\partial t} - V \frac{\partial C}{\partial z} = D \left( \frac{\partial^2 C}{\partial x^2} + \frac{\partial^2 C}{\partial z^2} \right).$$

Now this equation is further subject to the boundary conditions

$$\begin{aligned} T &= T_L \left( \frac{C_0}{k_D} \right) - m \left( C - \frac{C_0}{k_D} \right) - \Gamma \nabla \cdot \underline{n} \quad (z = \eta). \\ (1 - k_D)C \left( V + \frac{\partial \eta}{\partial t} \right) &= -D \frac{\partial C}{\partial z} \quad (z = \eta). \\ C &\rightarrow C_0 \quad (z \rightarrow \infty) \end{aligned} \tag{17}$$

The first condition is the interfacial temperature condition including the Gibbs-Thomson effect. The next condition is the concentration condition (analogous to the Stefan condition). The last condition sets the concentration far from the interface. Inserting the concentration field, equation (16), into the advection-diffusion equation, noting that the base case will cancel by definition, we have

$$\frac{V^2}{D} \sigma \hat{\phi} e^{i\alpha \frac{Vx}{D} + \sigma \frac{V^2}{D} t} - \frac{V^2}{D} \hat{\phi}' e^{i\alpha \frac{Vx}{D} + \sigma \frac{V^2}{D} t} = D \left( -\frac{V^2}{D^2} \alpha^2 \hat{\phi} e^{i\alpha \frac{Vx}{D} + \sigma \frac{V^2}{D} t} + \frac{V^2}{D^2} \hat{\phi}'' e^{i\alpha \frac{Vx}{D} + \sigma \frac{V^2}{D} t} \right).$$

Canceling the exponential and constant factors and we arrive at

$$\sigma \hat{\phi} - \hat{\phi}' = -\alpha^2 \hat{\phi} + \hat{\phi}''.$$

Hypothesizing a solution of the form

$$\hat{\phi} = \hat{\phi}_0 e^{-\mu z},$$

because it must behave at infinity and zero, we determine that

$$\mu^2 - \mu - (\sigma + \alpha^2) = 0.$$

From the quadratic formula, we get the condition that

$$\mu = \frac{1}{2} \left[ 1 + \sqrt{1 + 4(\sigma + \alpha^2)} \right].$$

Hence, the concentration profile can then be written as

$$C = C_0 + \left( \frac{1 - k_D}{k_D} \right) C_0 e^{-\frac{V}{\kappa} z} + \hat{\phi}_0 e^{i\alpha \frac{Vx}{D} - \mu \frac{Vz}{D} + \sigma \frac{V^2}{D} t}.$$

This equation and the temperature profile can then be inserted into the interfacial temperature condition. To do this, since the condition applies at  $z = \eta$ , we will Taylor expand everything about  $z = 0$ . Furthermore, for the Gibbs-Thomson effect, the curvature is need. As computed before,

$$\nabla \cdot \underline{n} \simeq -\frac{\partial^2 \eta}{\partial x^2}.$$



Thus, the temperature interface condition yields

$$T_0 + \frac{\partial T}{\partial z} \eta = T_0 - m \left( C(0) + \frac{\partial C}{\partial z} \Big|_0 \eta - \frac{C_0}{k_D} \right) - \Gamma \frac{\partial^2 \eta}{\partial z^2}.$$

Canceling the common terms and inserting the definitions of  $\eta$ ,  $T$ , and  $C$  (and removing the exponentials) we obtain

$$G\hat{\eta} = -m \left( C_0 + \left( \frac{1-k_D}{k_D} \right) C_0 + \hat{\phi}_0 - \frac{V}{D} \left( \frac{1-k_D}{k_D} \right) C_0 \hat{\eta} - \frac{C_0}{k_D} - \mu \frac{V}{D} \hat{\eta} \hat{\phi}_0 e^{i\alpha \frac{Vx}{D} - \mu \frac{Vz}{D} + \sigma \frac{V^2}{D} t} \right) - \alpha^2 \Gamma \frac{V^2}{D^2} \hat{\eta}.$$

The last term in the brackets can be dropped because it is second order in the perturbation quantity. Furthermore, several terms involving  $C_0$  and  $k_D$  can be canceled. This yields the much more manageable expression

$$G\hat{\eta} = -m\hat{\phi}_0 + m\frac{V}{D} \left( \frac{1-k_D}{k_D} \right) C_0 \hat{\eta} - \alpha^2 \Gamma \frac{V^2}{D^2} \hat{\eta}.$$

Now we can define the dimensionless solute gradient  $G_C$  to be

$$G_C = -\frac{V}{D} \left( \frac{1-k_D}{k_D} \right) C_0.$$

Thus, with some rearranging we have

$$\boxed{\left( G + mG_C + \alpha^2 \frac{V^2}{D^2} \Gamma \right) \hat{\eta} = -m\hat{\phi}_0.}$$

Now the same procedure can be perform for the concentration condition, although it is a little more involved. Writing the condition and Taylor expanding around  $z = 0$ , we have

$$(1-k_D) \left( C(0) + \frac{\partial C}{\partial z} \Big|_0 \eta \right) \left( V + \frac{\partial \eta}{\partial t} \right) = -D \left( \frac{\partial C}{\partial z} \Big|_0 + \frac{\partial^2 C}{\partial z^2} \Big|_0 \eta \right).$$

Inserting the definition of  $C$  and  $\eta$  and keeping only first order terms we have

$$(1-k_D) \left( \frac{C_0}{k_D} + \hat{\phi}_0 - \frac{V}{D} \left( \frac{1-k_D}{k_D} \right) C_0 \hat{\eta} \right) \left( V + \frac{V^2}{D} \sigma \hat{\eta} \right) = V \left( \frac{1-k_D}{k_D} \right) C_0 + V \mu \hat{\phi}_0 - \frac{V^2}{D} \left( \frac{1-k_D}{k_D} \right) C_0 \hat{\eta}.$$

Canceling a  $V$  from all of the terms, evaluating the left side to first order, and canceling terms that appears on both sides we have

$$\left( \frac{1-k_D}{k_D} \right) C_0 \frac{V}{D} \sigma \hat{\eta} + \hat{\phi}_0 (1-k_D) + k_D \frac{V}{D} \left( \frac{1-k_D}{k_D} \right) C_0 \hat{\eta} = \mu \hat{\phi}_0.$$

The definition of the solute gradient  $G_C$  can then be put in this last expression to yield

$$-G_C \sigma \hat{\eta} + \hat{\phi}_0 (1-k_D) - k_D G_C \hat{\eta} = \mu \hat{\phi}_0.$$

Rearranging we have that

$$\boxed{-G_C(k_D + \sigma) \hat{\eta} = (\mu - 1 + k_D) \hat{\phi}_0.}$$

Now the simplified interfacial temperature condition and the concentration condition at the interface (the two boxed equations) can be combined to give

$$mG_C(k_D + \sigma) = (\mu - 1 + k_D) \left( G + mG_C + \alpha^2 \frac{V^2}{D^2} \Gamma \right).$$

Dividing through and solving for  $\sigma$  we find that

$$\sigma = -k_D + (\mu - 1 + k_D) \left( 1 + \frac{G}{mG_C} + \frac{\alpha^2 V^2 \Gamma}{mD^2 G_C} \right).$$

Now defining three new groups we have

$$M = -\frac{mG_C}{G},$$

which is the *morphological number* and

$$L_C = \frac{D}{V},$$

the diffusion lengthscale, and the capillary length,  $L_\Gamma$ , given by

$$L_\Gamma = \frac{\Gamma k_D}{mC_0(1 - k_D)} = -\frac{V\Gamma}{mDG_C}.$$

Thus, we have that

$$\sigma = -k_D + (\mu - 1 + k_D) \left( 1 - M^{-1} - \alpha^2 \frac{L_\Gamma}{L_C} \right).$$

## 10 Lecture on 19 February 2013

### 10.1 Morphological Instability *continued*

Starting with the dispersion relation derived in the last lecture, marginal stability occurs for  $\sigma = 0$ . Also, the key features occur when  $\alpha \gg 1$ , with  $\sigma \sim O(\alpha)$  and  $\mu \sim \alpha$ . Furthermore,  $\mu \gg k_d$ . Thus, we can write

$$k_D = \alpha \left( 1 - M^{-1} - \alpha^2 \frac{L_\Gamma}{L_C} \right).$$

Thus, we can solve for  $M^{-1}$  as

$$M^{-1} = 1 - \frac{k_D}{\alpha} - \alpha^2 \frac{L_\Gamma}{L_C}.$$

The minimum value of  $M$  for which morphological instability can occur is found by taking the derivative of  $M^{-1}$  with respect to  $\alpha$  and setting this equal to zero. Thus,

$$\frac{\partial M^{-1}}{\partial \alpha} = \frac{k_D}{\alpha^2} - 2\alpha \frac{L_\Gamma}{L_C} = 0 \longrightarrow \alpha_{cr} = \left( \frac{k_D L_C}{2L_\Gamma} \right)^{\frac{1}{3}}.$$

Taking another derivative and inserting  $\alpha_{cr}$ , we have

$$\left. \frac{\partial^2 M^{-1}}{\partial \alpha^2} \right|_{\alpha_{cr}} = -\frac{2k_D}{\alpha_{cr}^3} - 2\frac{L_\Gamma}{L_C} = -6\frac{L_\Gamma}{L_C},$$

which is a maximum of  $M^{-1}$  and thus a minimum of  $M$ . Plugging  $\alpha_{cr}$  into the expression for  $M^{-1}$  we have that

$$M_{cr}^{-1} = 1 - k_D \left( \frac{2L_\Gamma}{k_D L_C} \right)^{\frac{1}{3}} - \left( \frac{k_D L_C}{2L_\Gamma} \right)^{\frac{2}{3}} \frac{L_\Gamma}{L_C} = 1 - \left( \frac{8k_D^2 L_\Gamma}{4L_C} \right)^{\frac{1}{3}} - \left( \frac{k_D^2 L_\Gamma}{4L_C} \right)^{\frac{1}{3}}.$$

Thus, the minimum value of  $M$  for morphological instability is

$$M_{cr}^{-1} = 1 - \frac{3}{2} \left( \frac{2k_D^2 L_\Gamma}{L_C} \right)^{\frac{1}{3}}.$$

Thus, for instability we need  $M > M_{cr} > 1$ . This is a stricter condition than imposed by constitutional supercooling due to the Gibbs-Thomson effect. In terms of lab parameters we have that

$$\frac{D}{V} \frac{Gk_D}{C_0(1 - k_D)} = 1 - \frac{3}{2} \left( 2k_D^2 \frac{\Gamma k_D}{mC_0(1 - k_D)} \frac{V}{D} \right)^{\frac{1}{3}},$$

where  $G$  is the slope of the temperature base state,  $\Gamma$  is the coefficient from the Gibbs-Thompson effect,  $C_0$  is the concentration of solute in the solid,  $V$  is the solidification speed,  $D$  is the diffusivity of solute,  $k_D$  is the distribution coefficient, and  $m$  is the liquidus slope.

## 11.1 Mushy Layers

Here we describe the formation of layers between solid and liquid where dendritic crystals form and give rise to a porous medium. In this section we seek a description of the mushy layer that is “averaged” and independent of the microscopic morphology and depends only on

$$\begin{aligned} T(\underline{x}, t) &:: \text{Local Mean Temperature,} \\ C(\underline{x}, t) &:: \text{Local Mean Concentration in liquid,} \\ \phi(\underline{x}, t) &:: \text{Local Mean Volume fraction of } \textit{solid}. \end{aligned}$$

Here it is important to note that  $\phi$  does not need to be continuous from the solid to the liquid. If there is no mushy layer, then there is a discontinuity in  $\phi$  from 0 in the liquid to 1 in the solid.

As part of the definition of the mushy layer we will assume that the solid phase is stationary. Drawing an infinitesimal control volume that is large enough to contain representative samples of both phases, we can write *conservation of mass* as

$$\frac{d}{dt} \int_{\mathcal{D}} \bar{\rho} dV = - \int_{\partial \mathcal{D}} \rho_l \underline{u} \cdot \underline{n} dS.$$

Here  $\mathcal{D}$  is the control volume. The average density is given as

$$\bar{\rho} = \phi \rho_s + (1 - \phi) \rho_l.$$

The velocity is the Darcy velocity, which is the volume flux of liquid per unit area of mush, which is given as

$$\underline{u} = (1 - \phi) \underline{u}_I,$$

where  $\underline{u}_I$  is the mean interstitial fluid velocity. Combining the two integrals into a single integral we have that

$$\int_{\mathcal{D}} \frac{\partial \bar{\rho}}{\partial t} + \nabla \cdot (\rho_l \underline{u}) dV = 0.$$

Because the control volume is arbitrary we can write

$$\frac{\partial \bar{\rho}}{\partial t} + \nabla \cdot (\rho_l \underline{u}) = 0.$$

If the solid density  $\rho_s$  and the liquid density  $\rho_l$  are assumed to be constant, which is the Boussinesq approximation, we can write

$$\nabla \cdot \underline{u} = (1 - r) \frac{\partial \phi}{\partial t} \quad \text{where} \quad r = \frac{\rho_s}{\rho_l}.$$

If ice is growing in water, since the density of ice is less than that of water,  $\rho_s < \rho_l$  and the rate of change of the solid fraction with time is positive  $\partial \phi / \partial t > 0$ , this means that  $\nabla \cdot \underline{u} > 0$ . When  $r < 1 \leftrightarrow \rho_s < \rho_l$ , the mixture expands on freezing. There is a positive divergence when the volume fraction of solid grows with time. This is the case of “brine expulsion” in sea ice but in fact it is not entirely true. It turns out that this can only redistribute salt and, for example, deepen a layer of sea ice — it doesn’t eject salt into the ocean. A common approximation is to set  $r = 1 \leftrightarrow \rho_s = \rho_l$ .

Following a similar derivation from the beginning of the class and mimicking the averaged analysis performed for the conservation of mass, we can find *heat conservation* to be

$$\overline{\rho \mathcal{C}_p} \frac{\partial T}{\partial t} + \rho_l \mathcal{C}_{p_l} \underline{u} \cdot \nabla T = \nabla \cdot (\bar{k} \nabla T) + \rho_s \mathcal{L} \frac{\partial \phi}{\partial t}.$$

The *latent heat*,  $\mathcal{L} = H_l - H_s$ , is the difference between the sensible heat in the liquid and solid and is a function of the local concentration and temperature. However, if the phase change inside the mushy layer is at equilibrium then the temperature is the liquidus temperature,  $T = T_L(C)$ , and therefore the latent heat only a function of the concentration. Usually the latent heat is a constant. The mean heat capacity per unit volume is given as

$$\overline{\rho \mathcal{C}_p} = \phi \rho_s \mathcal{C}_{p_s} + (1 - \phi) \rho_l \mathcal{C}_{p_l}.$$

This is an exact relationship because  $\rho$  and  $C_p$  are extensive properties, i.e., dependent on mass and volume. The heat conductance  $\bar{k}$  is a function of the local solid fraction and the internal morphology. For a laminated material with a thermal gradient aligned with the sheets, gives an average heat conductance of

$$\bar{k}_{\parallel} = \phi k_s + (1 - \phi)k_l.$$

In the opposite case, when the thermal gradient is perpendicular to the sheets, we have that

$$\bar{k}_{\perp} = \frac{1}{\frac{\phi}{k_s} + \frac{1-\phi}{k_l}}.$$

These two definitions of the heat conductance are the upper and lower bounds for  $\bar{k}$  in an arbitrary media. Often we take  $\bar{k} = \bar{k}_{\parallel}$ , because the primary dendrites are aligned with the mean thermal gradient. If the thermal gradient changes direction, the growth of dendrites will adjust.

Conservation of solute gives the equation

$$(1 - \phi) \frac{\partial C}{\partial t} + \underline{u} \cdot \nabla C = \nabla \cdot (\bar{D} \nabla C) + r(1 - k_D)C \frac{\partial \phi}{\partial t}.$$

The distribution coefficient,  $k_D$  is the parameter that connects  $C$  and  $C_s$ , as  $C = k_D C_s$ . Furthermore, we usually take  $\bar{D} = (1 - \phi)D$ , as diffusion in the solid phase is negligible. Note that a common approximation is  $r = 1$ , which implies that the velocity field is *solenoidal* or divergence free. We also frequently set  $k_D = 0$ .

Thus, the equations we have derived so far are

$$\begin{aligned} \nabla \cdot \underline{u} &= 0, & (\text{mass conservation}) \\ \bar{\rho} C_p \frac{\partial T}{\partial t} + \rho_l C_{pl} \underline{u} \cdot \nabla T &= \nabla \cdot (\bar{k} \nabla T) + \rho_s \mathcal{L} \frac{\partial \phi}{\partial t}. & (\text{heat conservation}) \\ (1 - \phi) \frac{\partial C}{\partial t} + \underline{u} \cdot \nabla C &= \nabla \cdot [(1 - \phi)D \nabla C] + r(1 - k_D)C \frac{\partial \phi}{\partial t}. & (\text{solute conservation}) \end{aligned}$$

However, there are too many unknowns and not enough equations. We need an equation to describe the change in solid fraction.

### 11.1.1 Evolution of Solid Fraction

The terms proportional to  $\partial \phi / \partial t$  release heat and solute into the mushy layer. This release of heat increases  $T$  and the release of salt decreases  $T_L$  (liquidus temperature). Both of these effects reduce the level of conditional supercooling. Here we will assume that conditional supercooling is *entirely eliminated*. If there were any supercooling it would lead to further instabilities. Thus, the temperature throughout the mushy layer is equal to the liquidus temperature, i.e.,

$$\boxed{T = T_L(C).}$$

This reduces the order of the above equations from fourth order down to third order. This ties concentration and temperature together in the mushy layer and essentially they become a single variable.

## 12 Lecture on 26 February 2013

Starting from the mushy layer equations given in the last lecture, with the temperature in the mushy layer equal to the liquidus temperature, which connects temperature and solute concentration. This is called *corregating* and it is the process by which the temperature is increased (rate of release of latent heat) and the rate of release of salt is decreased. At the liquid/mush interface the temperature line and the liquidus temperature line meet without conditional supercooling. Furthermore, as we will see, the temperature line and liquidus temperature at *tangent* at the mushy layer and liquid interface.

### 12.1 Interfacial Conditions

To link the temperature, concentration, and flows in the different regions we must apply conditions at the interface. Conservation of mass gives

$$[\underline{u} \cdot \underline{n}] = -(1 - r)v_n[\phi].$$

The brackets indicate that the conditions are applied above and below the interface and equated. Conservation of heat gives the expression

$$\rho_s \mathcal{L} v_n[\phi] = [\bar{k} \underline{n} \cdot \nabla T].$$

This is essentially the Stefan condition across the interface. For the conservation of solute across the interface we can write

$$r(1 - k_D)C[\phi] = [\bar{D} \underline{n} \cdot \nabla C].$$

These equations are sufficient to determine  $T$  and  $C$  but an addition condition is needed for  $\phi$ .

### 12.1.1 Condition of Marginal Equilibrium

This is the constraint on the system that we can use to determine the solid fraction  $\phi$ . We assume that the mushy layer grows sufficiently to completely eliminate constitutional supercooling ahead of the mush-liquid interface. This means that, on the phase diagram, as the temperature cools it never dips below the liquidus temperature line. To make sure of this, we have the condition of marginal equilibrium given by

$$\left. \frac{\partial T}{\partial n} \right|_l = \left. \frac{\partial T_L}{\partial n} \right|_l,$$

at the mush-liquid interface. As a consequence we have that  $\phi = 0$  at the interface. This is a little surprising as  $\phi$  is an averaged quantity.

### 12.2 Conservation of Solute

In the mushy layer, solute does not need to be pushed ahead of the advancing interface but rather can be pushed out sideways. An underlying assumption that we employ here is that no solute can leave the region. Thus, we can write

$$\int_0^h (1 - \phi) C_L(T) dz = h C_0.$$

Here  $C_0$  is all of the solute (or salt) in the region. This condition comes directly from the conservation of solute expression given before, except  $k_D = 0$  and  $r = 1$ . Making a *quasi-stationary approximation*, which is okay for large Stefan numbers  $\mathcal{S}$ , we have that

$$T = T_B + (T_L(C_0) - T_B) \frac{z}{h}.$$

Because the temperature in the mushy layer is identical to the liquidus temperature we have that

$$T = T_L(C) \longleftrightarrow C = C_L(T),$$

and therefore we can write

$$C_L(T) = C_B + (C_0 - C_B) \frac{z}{h},$$

where we have defined  $C_B = C_L(T_B)$ . Inserting this into the solute conservation equation, and assuming that the solid fraction is not a function of  $z$ , we have that

$$\int_0^h (1 - \phi) \left( C_B + (C_0 - C_B) \frac{z}{h} \right) dz = h C_0.$$

Integrating and evaluating the endpoints we have that

$$(1 - \phi) \left( C_B h + (C_0 - C_B) \frac{h}{2} \right) = h C_0.$$

Here we can cancel the  $h$  factors and combine terms to find

$$(1 - \phi)(C_0 + C_B) = 2C_0.$$

Solving for  $\phi$  we obtain

$$\phi = \frac{C_B - C_0}{C_B + C_0}.$$

We can define a concentration number  $\mathcal{C}$  as

$$\mathcal{C} = \frac{C_0}{C_B - C_0}.$$

Note that this is different from the concentration number used in Batchelor et al. (2000). Thus, we can write the constant solid fraction as

$$\phi = \frac{1}{2\mathcal{C} + 1}.$$

A large concentration number implies that  $C_B - C_0$  and therefore the solid fraction is small. Ignoring the heat transfer in the liquid we can write the Stefan condition as

$$\phi \rho_s \mathcal{L} \dot{h} = \overline{k(\phi)} \left. \frac{\partial T}{\partial z} \right|_{h-}.$$

In the heat conductance term  $\overline{k(\phi)}$ , the solid fraction in parentheses is a reminder that it is a function of  $\phi$ , from here on it will be dropped however. Thus, using the quasi-stationary approximation we have that

$$\phi \rho_s \mathcal{L} \dot{h} = \bar{k} \frac{(T_L(C_0) - T_B)}{h}.$$

Multiplying the right side by  $k_s/k_s$  and using the fact that  $k_s = \rho_s \mathcal{C}_{ps} \kappa_s$ , we have

$$\frac{\rho_s \mathcal{L}}{\rho_s \mathcal{C}_{ps} (T_L(C_0) - T_B)} h \dot{h} = \frac{\bar{k}}{\phi k_s} \kappa_s.$$

We can simplify the collection of terms on the left side as a Stefan number

$$\mathcal{S} = \frac{\mathcal{L}}{\mathcal{C}_{ps} (T_L(C_0) - T_B)}.$$

Thus, we have that

$$h \dot{h} = \frac{\bar{k}}{\phi k_s} \mathcal{S} \kappa_s.$$

Integrating gives that the mushy layer thickness grows as

$$h = \sqrt{\frac{2\bar{k}}{\phi k_s \mathcal{S}} \kappa t}$$

This highlights the fact that the growth of the mushy layer is determined by the rate of *thermal* diffusion.

### 12.3 Reduced Equations for a Mushy Layer

The full equations for a mushy layer can be simplified under the following assumptions:

1. The density of the solid and liquid are identical,  $\rho_s = \rho_l \rightarrow r = 1$ .
2. Zero distribution coefficient,  $k_D = 0$ . This means that the solute concentration is zero in the solid.
3. The rate of solutal diffusion is much smaller than the rate of thermal diffusion,  $D \ll \kappa$ . This means that  $\epsilon^2 \ll 1$ .
4. Thermal properties such as  $k, \mathcal{C}_p$  are independent of phase and uniformly constant.

Thus, the equations for a mushy layer reduce to

$$\begin{aligned} \frac{\partial T}{\partial t} + \underline{u} \cdot \nabla T &= \kappa \nabla^2 T + \frac{\mathcal{L}}{\mathcal{C}_p} \frac{\partial \phi}{\partial t}, & (\text{heat conservation}) \\ (1 - \phi) \frac{\partial C}{\partial t} + \underline{u} \cdot \nabla C &= C \frac{\partial \phi}{\partial t}, & (\text{solute conservation}) \\ T &= T_L(C), & (\text{marginal equilibrium}) \\ \nabla \cdot \underline{u} &= 0. & (\text{mass conservation}) \end{aligned}$$

If there is no flow, i.e.,  $\underline{u} = 0$ , solute conservation gives that

$$(1 - \phi) \frac{\partial C}{\partial t} = C \frac{\partial \phi}{\partial t} \longrightarrow \frac{\partial}{\partial t} [(1 - \phi)C].$$

This means that the quantity  $(1 - \phi)C$  is independent of time, and therefore we can write

$$(1 - \phi)C = C_B(\underline{x}),$$

where these quantities are time independent and  $C_B$  is the bulk concentration. If the melt is uniform, we have that  $C_B = C_0 = \text{constant}$ . Thus, locally, for a uniform melt

$$\phi = 1 - \frac{C_0}{C_L(T)}.$$

### 13 Lecture on 28 February 2013

For a uniform melt with no flow, in the last lecture we derived the expression

$$\phi = 1 - \frac{C_0}{C_L(T)}.$$

Taking a derivative with respect to time we have that

$$\frac{\partial \phi}{\partial t} = \frac{C_0}{C_L(T)^2} \frac{\partial C}{\partial t}.$$

Because  $T = T_L(C)$ , we have that

$$\frac{\partial \phi}{\partial t} = \frac{C_0}{C_L(T)^2} \frac{\partial C}{\partial t} = \frac{C_0 C_L(T)'}{C_L(T)^2} \frac{\partial T}{\partial t}.$$

We can then insert this into the heat conservation equation without flow, to find that

$$\frac{\partial T}{\partial t} = \kappa \nabla^2 T + \frac{\mathcal{L}}{\mathcal{C}_p} \left( \frac{C_0 C_L(T)'}{C_L(T)^2} \right) \frac{\partial T}{\partial t}.$$

Rearranging gives

$$\left[ 1 + \frac{\mathcal{L}}{\mathcal{C}_p} \frac{C_0 (-C_L(T)')}{C_L(T)^2} \right] \frac{\partial T}{\partial t} = \kappa \nabla^2 T.$$

The quantity in brackets can be called  $\mathcal{C}'(T)$ . Thus, we have a nonlinear diffusion equation given as

$$\mathcal{C}'(T) \frac{\partial T}{\partial t} = \kappa \nabla^2 T.$$

This shows that the internal release of latent heat contributes to the effective heat capacity of the medium — latent heat acts as an additional *thermal inertia*. Structurally this equation is the same as the previous diffusion equations:  $\mathcal{C}'(T)$  has no length information and therefore this equation admits a similarity solution. We find that  $h \sim \sqrt{\kappa t}$ . The situation is that inside the mushy layer, the temperature evolves according to the nonlinear diffusion equation, and the solid fraction is given as

$$\phi = 1 - \frac{C_0}{C_L(T)}.$$

In the liquid region, the temperature profile is governed by the standard diffusion equation with no flow, i.e.,

$$\frac{\partial T}{\partial t} = \kappa \nabla^2 T.$$

At the interface we have that

$$T = T_L(C_0) \rightarrow C_L(T) = C_0.$$

Together with the solid fraction relationship, we can see explicitly that  $\phi = 0$  at the interface and that there is *no additional release of latent heat*. The Stefan condition gives

$$0 = \left[ k \frac{\partial T}{\partial z} \right],$$

so that there is no jump in gradient/slope.

### 13.1 Flow Inside a Mushy Layer

We treat the mushy layer as a porous medium with  $\underline{u}$  satisfying Darcy's equation

$$\mu \underline{u} = \Pi(\phi) [-\nabla p + (\rho - \rho_0)g].$$

Here  $\Pi(\phi)$  is the permeability. The density is a function of the density and the solute concentration and thus for this two component system, we can write a linear dependence as

$$\rho = \rho_0 [1 - \alpha(T - T_0) + \beta(C - C_0)].$$

Two components can lead to double diffusion effects but the liquidus constraint,  $T + T_L(C_0)$  ties them together. Assuming a locally linear liquid gives

$$T_L(C) = T_L(C_0) - m(C - C_0).$$

Calling  $T_0 = T_L(C_0)$ , we can write

$$\rho = \rho_0 [1 + \beta^*(C - C_0)],$$

where

$$\beta^* = \beta + m\alpha.$$

When temperature effects are small, we have that  $\beta^* \simeq \beta$ . Defining a dimensionless variable for the temperature and concentration we have that

$$\theta = \frac{T - T_0}{T_0 - T_B} = \frac{C - C_0}{C_0 - C_B} \quad \text{with} \quad T_I = T_L(C_I), \quad (\text{at interface})$$

For zero distribution coefficient, we have the equations

$$\begin{aligned} \frac{\partial \theta}{\partial t} + \underline{u} \cdot \nabla \theta &= \kappa \nabla^2 \theta + \mathcal{S} \frac{\partial \phi}{\partial t}, \\ (1 - \phi) \frac{\partial \theta}{\partial t} + \underline{u} \cdot \nabla \theta &= -(\mathcal{C} - \theta) \frac{\partial \phi}{\partial t}, \\ \underline{u} &= -\frac{\Pi}{\mu} [\nabla p + \rho_0 \beta^* \Delta C \theta \underline{g}]. \end{aligned}$$

Here we have combined terms using the following groupings

$$\mathcal{S} = \frac{\mathcal{L}}{\mathcal{C}_p \Delta T}, \quad \mathcal{C} = \frac{C_0}{\Delta C}, \quad \Delta T = T_0 - T_B = m \Delta C, \quad \text{and} \quad \Delta C = C_B - C_0.$$

#### 13.1.1 Near-Eutectic Approximation

Now we will employ the *near-eutectic approximation*, which means that  $\mathcal{C} \gg 1$ , and  $\Delta C$  is small compared to  $C_0$ , or  $\Delta C \ll C_0$ . For very large concentration ratios,  $\mathcal{C} \gg 1$ , the solid fraction  $\phi$  is small,  $\phi \ll 1$ . This can be seen from the no flow expression

$$\phi = \frac{1}{2\mathcal{C} + 1}.$$

This is a better approximation for sodium acetate than it is for sea ice. Thus, from the equations above, the two terms

$$(1 - \phi) \quad \text{and} \quad (\mathcal{C} - \theta),$$

can be simplified to give the ratio

$$\frac{1 - \phi}{\mathcal{C} - \theta} \simeq \frac{1}{\mathcal{C}}.$$

Thus, the solutal conservation equation gives

$$\frac{D\theta}{Dt} = \frac{\partial \theta}{\partial t} + \underline{u} \cdot \nabla \theta = -\mathcal{C} \frac{\partial \phi}{\partial t}.$$



Eliminating  $\phi$  from the above equations we have that

$$\left[ 1 + \frac{\mathcal{S}}{\mathcal{C}} \right] \frac{D\theta}{Dt} = \kappa \nabla^2 \theta \quad \text{and} \quad \underline{u} = -\frac{\Pi}{\mu} [\nabla p + \rho_0 \beta^* \Delta C \theta \underline{g}].$$

The extra term in front of the total derivative of  $\theta$  is the enhancement of specific heat due to a release of latent heat. By making these approximations, we have taken the equations for a reactive porous medium and simplified them to equations for a passive porous medium. Using these equation we can describe convection in a passive porous medium.

### 13.2 Onset of Convection in a Horizontal Mushy Layer

Consider the convection between two flat plates, the bottom one at  $z = 0$  and the top one at  $z = h$ . The temperature conditions at the top and bottom are  $T_0$  and  $T_B$  respectively. This gives the boundary conditions

$$\theta(z = 0) = -1 \quad \text{and} \quad \theta(z = h) = 0.$$

The flow in the layer is two dimensional with components  $\underline{u} = (u, w)$ . The unit vector  $\hat{k}$  points vertically up and the gravity vector is equal to  $\underline{g} = -g\hat{k}$ . We can scale the equations to make them nondimensional. We scale lengths by  $h$ , time by  $h^2\Omega/\kappa$ , velocity by  $\kappa/h\Omega$ , and pressure by  $\beta^*\Delta C\rho_0gh$ , where  $\Omega = 1 + (\mathcal{S}/\mathcal{C})$  and  $\kappa$  is the thermal diffusivity. This gives the nondimensionalized equations

$$\frac{\partial \theta}{\partial t} + \underline{u} \cdot \nabla \theta = \nabla^2 \theta \quad \text{and} \quad \underline{u} = -R_m [\nabla p - \theta \hat{k}], \quad \text{where} \quad R_m = \frac{\beta^* \Delta C g \Pi h}{\kappa \nu} \Omega.$$

Here  $R_m$  is the porous medium Raleigh number. The permeability  $\Pi$  gives the dissipation on the pore scale and the  $h$  comes from potential energy. The buoyancy comes from the  $\Delta C$ , which is *solutal buoyancy*, but it is set by the thermal diffusivity,  $\kappa$ . This porous medium Raleigh number relates the solutal buoyancy to the thermal dissipation with enhanced specific heat, due to internal latent heat release (which is the effect of  $\Omega$ ), and diminishes the thermal diffusivity.

The basic state is in steady state, horizontally homogeneous, and has  $\underline{u} = 0$ . Thus, we have

$$\frac{\partial^2 \theta}{\partial z^2} = 0 \longrightarrow \theta = Az + B \longrightarrow \theta = z - 1,$$

where the scaled boundary conditions are now  $\theta(z = 0) = -1$  and  $\theta(z = 1) = 0$ .

## 14 Lecture on 5 March 2013

### 14.1 Onset of Convection in a Horizontal Mushy Layer *continued*

The basic state for convection in a mushy layer was derived at the end of the last lecture and is given by  $\underline{u} = 0$  and  $\theta = z - 1$ , under scaled coordinates where  $z \in [0, 1]$ . Using a streamfunction,  $\psi$ , we can write the perturbation velocity as

$$\underline{u}' = \left( \frac{\partial \psi}{\partial z}, -\frac{\partial \psi}{\partial x} \right).$$

The total nondimensional heat and solute,  $\theta$ , is given as the basic state plus the perturbation as

$$\theta = -1 + z + \theta',$$

where the primes on the perturbation variables indicate that they are small, and not that they are derivatives. Inserting these quantities into the nondimensional thermal conservation equation we have that

$$\nabla^2 \theta' = \frac{\partial \theta'}{\partial t} + \frac{\partial \psi}{\partial z} \frac{\partial}{\partial x} (-1 + z + \theta') - \frac{\partial \psi}{\partial x} \frac{\partial}{\partial z} (-1 + z + \theta').$$

We have canceled the basic state because it satisfies the equation by definition. This can be linearized, where products of perturbations are neglected, as

$$\nabla^2 \theta' = \frac{\partial \theta'}{\partial t} - \frac{\partial \psi}{\partial x}.$$

Inserting the perturbation velocity into Darcy's equation gives

$$\nabla \wedge (\psi \hat{j}) = -R_m \nabla \wedge [\nabla p - \theta \hat{j}].$$

The vertical components, proportional to  $\hat{k}$ , have be switched to  $\hat{j}$  to make the cross products work out in the 3D matrix form. Computing it out we find that

$$\nabla^2 \psi = -R_m \frac{\partial \theta'}{\partial x},$$

because the pressure cancels, as gradient fields are curl free. Thus, all of the equations and boundary conditions are

$$\begin{aligned} \nabla^2 \theta' &= -\frac{\partial \psi}{\partial x} + \frac{\partial \theta}{\partial t}, \\ \nabla^2 \psi &= -R_m \frac{\partial \theta}{\partial x}, \\ \theta' &= \psi = 0 \quad \text{on} \quad z = 0, 1. \end{aligned}$$

We can look for normal mode solutions of the form

$$\theta' = \hat{\theta}(z) e^{i\alpha x + \theta t} \quad \text{and} \quad \psi = \hat{\psi}(z) e^{i\alpha x + \theta t}.$$

Marginal equilibrium occurs at  $\sigma = 0$ . There are eigensolutions to these equations of the form

$$\hat{\theta}(z) = A_n \sin(\pi n z) \quad \text{and} \quad \hat{\psi}(z) = B_n \cos(\pi n z).$$

Inserting the normal mode solutions with these eigensolution amplitudes, into the linearized equations, we have that

$$(-n^2 \pi^2 - \alpha^2) A_n = -i\alpha B_n \quad \text{and} \quad (-n^2 \pi^2 - \alpha^2) B_n = -i\alpha R_m A_n.$$

Solving for  $R_m$ , we find that

$$-R_m = \frac{[(n\pi)^2 + \alpha^2]^2}{\alpha^2}.$$

The first instability occurs for  $n = 1$ , and thus, instabilities occur when,

$$-R_m > \frac{(\pi^2 + \alpha^2)^2}{\alpha^2}.$$

The minus sign is because  $g\Delta C < 0$ . Taking a derivative, we find that

$$-\frac{\partial R_m}{\partial \alpha} = \frac{4\alpha(\pi^2 + \alpha^2)}{\alpha^2} - \frac{2(\pi^2 + \alpha^2)^2}{\alpha^3} = 0,$$

which means that

$$4\pi^2 \alpha^2 + 4\alpha^4 = 2\pi^4 + 4\pi^2 \alpha^2 + 2\alpha^4 \longrightarrow \alpha_{cr} = \pi.$$

This gives a minimum critical Raleigh number of

$$\boxed{-R_{m_{cr}} = 4\pi^2.}$$

Thus, convection occurs for

$$-\frac{\beta^* \Delta C g \Pi h \Omega}{\kappa \nu} > 4\pi^2.$$

Returning to the reason why the Raleigh number is negative, this situation corresponds to cooling from below with light solute release, where salt is crystallizing from solution. This could also be the case where there is cooling from above with heavy solute release, like sea ice.

Considering another boundary condition, we have that the top of the mushy layer, where there is contact with the liquid, is better approximated by a condition of constant pressure. In the liquid the dissipation occurs on the macroscale but in the mushy layer the dissipation occurs on the microscale, the pore scale. The velocity is continuous across the interface and relative to the porous medium, we don't need large pressure gradients in the liquid region. Computing the critical Rayleigh number in this scenario gives

$$-R_m \simeq 27.1,$$

which is less than  $4\pi^2$ , which we determined from the other analysis. Some notes on these solutions are

1. Convection is determined by the porous media Rayleigh number

$$R_m = \frac{\beta^* \Delta C g \Pi h \Omega}{\kappa \nu},$$

which is dependent on solutal buoyancy but thermal diffusivity.

2. Critical condition modified by a factor  $\Omega = 1 + \frac{\mathcal{S}}{\mathcal{C}}$ . This means that large latent heat, or large  $\mathcal{S}$ , means the configuration is more unstable to convection.

### 14.1.1 Parcel Argument

To help explain the two notes to the solution we think of the buoyant residual, less salty, and we are on the right hand of the binary phase diagram. Consider a parcel of fluid that is cold but fresh. It displaced up due to its lower buoyancy and thermal diffusion allows it to quickly equilibrate to the local temperatures. Since the diffusion of solute is much slower, the parcel is not fully equilibrated to the local solutal concentration, and thus remains relatively fresh. Then, this relatively fresh parcel dissolves the dendrites, the solid phase of mushy layer, in its new environment, which makes the parcel saltier. This entire process occurs on a thermal diffusion timescale. Thus, the dissipation of buoyancy happens on a thermal timescale and hence the reason for  $\kappa$  in  $R_m$ .

The large Stefan number implies that a lot of latent heat is needed to generate a phase change, so the mushy layer is less reactive. Thus, buoyancy is dissipated less efficiently and therefore is more unstable. From solute conservation we have that

$$\frac{\partial \phi}{\partial t} = -\frac{1}{\mathcal{C}} \frac{D\theta}{Dt},$$

which means that there is a flow component parallel to the temperature gradient that exceeds the speed of the isotherms. There is internal dissolution when the temperature of a fluid parcel increases. For high Rayleigh number flows, more freshwater enters the mushy layer and then solidifies. This decreases the porosity, which decreases the Rayleigh number.

## 15 Lecture on 7 March 2013

### 15.1 Interfacial Premelting

The state, solid or liquid, of a substance can be affected by the proximity of another substance. An example is of ice and air: for a solid block of ice below air, there is a layer of *melted water*, that separates the two.

#### 15.1.1 Van Der Waals Interactions

Molecules have an attractive force between them resulting from quantum mechanical fluctuations in the dipole moment of one molecule inducing sympathetic fluctuations in the other. The electric potential is given as

$$\varphi = -\frac{k_{12}}{R^6},$$

where  $k_{12}$  is a constant that describes the strength of the attraction between the two materials and  $R$  is the distance between them. For the interaction between a single molecule and a semi-infinite solid we have

$$\varphi = \int_D \frac{-\rho_1 k_{12}}{[r^2 + (h+z)^2]^3} dV$$

Integrating over half-space in cylindrical polars we have

$$\varphi = \int_0^\infty \int_0^{2\pi} \int_0^\infty \frac{-\rho_1 k_{12}}{[r^2 + (h+z)^2]^3} r dr d\theta dz.$$

Using a substitution for  $r$  we can integrate to find that

$$\varphi = \int_0^\infty \int_0^{2\pi} \frac{\rho_1 k_{12}}{4(h+z)^4} d\theta dz.$$

Integrating over  $\theta$  we find that

$$\varphi = \int_0^\infty \frac{\pi \rho_1 k_{12}}{2(h+z)^4} d\theta dz = -\frac{\pi}{6} \frac{\rho_1 k_{12}}{h^2}.$$

The density,  $\rho_1$ , is the number of molecules per unit volume. In a similar way we can compute the interaction between two infinite slabs (per unit area). All molecules in the upper slab interact with the molecules in the lower slab and the two slabs are separated by a distance  $d$ . Their densities are  $\rho_2$  for the top and  $\rho_1$  for the bottom. Thus, we can compute the total potential as

$$\varphi = \int_0^\infty -\frac{\pi}{6} \frac{\rho_1 \rho_2 k_{12}}{(z+d)^3} dz = -\frac{A_{12}}{12\pi d^2}.$$

The parameter  $A_{12}$  is called the *Hamaker Constant* and is a material dependent property that is given by

$$A_{12} = \pi^2 k_{12} \rho_1 \rho_2.$$

The attractive force per unit area in can then be calculated as

$$P_{vdw} = -\nabla \varphi = -\frac{A_{12}}{6\pi d^3}.$$

Now we can fill the thickness  $d$  with liquid. In this case there is a repulsive force, called the *disjoining force*, that is given by

$$P_T = \frac{A}{6\pi d^3} \quad \text{where} \quad A = A_{1l} + A_{2l} - A_{12} - A_{ll}. \quad (\text{thermomolecular pressure})$$

The subscript  $l$  stands for the liquid. If there is no liquid then the first two and last components of  $A$  are zero and we have the expression from before.

## 15.2 Premelting

Consider a substrate with force  $P_s$  and a solid block of ice with force  $P_s$ . Between these two is a layer of water with force  $P_l$ . Thus, a total balance of forces gives

$$P_s = P_l + P_T,$$

where  $P_T$  is the disjoining force. Now from the ClausiusClapeyron relation we have that

$$\begin{cases} \rho_s \mathcal{L} \frac{T_m - T}{T_m} = P_s - P_l & \text{if } \rho_s = \rho_l \\ \rho_s \mathcal{L} \frac{T_m - T}{T_m} = P_s - P_l + (P_s - P_m) \left( \frac{1}{\rho_s} - \frac{1}{\rho_l} \right) & \text{if } \rho_s \neq \rho_l \end{cases}$$

The  $P_s - P_l$  gave rise to the Gibbs-Thomson effect due to surface tension at curved surfaces. Thus, in equilibrium, for  $\rho_s = \rho_l$ , we have that

$$\rho_s \mathcal{L} \frac{T_m - T}{T_m} = P_s - P_l = P_T = \frac{A}{6\pi d^3}.$$

Rearranging we have that the distance,  $d$ , is given as

$$d = \left( \frac{AT_m}{6\pi \rho_s \mathcal{L}} \right)^{\frac{1}{3}} (T_m - T)^{-\frac{1}{3}}.$$

We can see that melting is a surface nucleated process and that the thickness decreases with undercooling. For ice in contact with vapor water at  $T = -1^\circ\text{C}$  has a thickness  $d \simeq 3.5 \times 10^{-9}$  m or 3.5 nm.

### 15.3 Lateral Heave in a Capillary Tube

Here we examine a long finger of ice in between two close fitting plates filled with water. In front of the ice there is only water. If the plates are solid there is a long thin flow between the plates and the ice. If the plates are elastic, for example consider an elastic tube filled with an icicle and water. The front of the icicle sucks water in and begins to freeze it. The freezing solid expands the tube, which it can do because it is elastic. Considering a temperature profile that decreases linearly away from the tip of the ice, we have a large disjoining force far from the tip, but the liquid pressure is low. Near the tip, the disjoining force is small but the liquid force is high.

## 16 Lecture on 12 March 2013

### 16.1 Lateral Heave in a Capillary Tube *continued*

Continuing with the problem of the ice in the elastic tube. The radius of the tube is at  $b(x, t)$ . If we consider that the tube is only susceptible to *hoop-stress*, and not a bending stress, we can write the solid force as

$$P_s = k(b - b_0) \quad \text{where} \quad k = \text{elastic constant.}$$

Also,  $b_0$  is the relaxed position of the tube. The liquid force is then

$$P_l = P_s - P_T = k(b - b_0) - \frac{\rho_s \mathcal{L}}{T_m} (T_m - T).$$

We also have that

$$T = T_m - mx \quad \text{and} \quad d = \Gamma (T_m - T)^{-\frac{1}{3}} \quad \text{where} \quad \Gamma = \left( \frac{AT_m}{6\pi\rho_s \mathcal{L}} \right)^{\frac{1}{3}}.$$

The coordinate  $x$  is positive along away from the tip along the ice opposite from the water. From *Lubrication Theory*, we can determine the volume flux, which is

$$q = 2\pi b_0 \frac{d^3}{12\mu} \left( -\frac{\partial P_l}{\partial x} \right).$$

From conservation of mass we have that

$$2\pi b_0 \frac{\partial b}{\partial t} + \frac{\partial q}{\partial x} = 0.$$

Inserting  $q$  and  $d$  into this expression we find that

$$\frac{\partial b}{\partial t} = \frac{\Gamma^3}{12\mu} \frac{\partial}{\partial x} \left\{ \frac{1}{(T_m - T)} \frac{\partial}{\partial x} \left[ k(b - b_0) - \frac{\rho_s \mathcal{L}}{T_m} (T_m - T_0) \right] \right\}.$$

If we consider  $T = T_m - mx$  to be fixed we have that

$$\frac{\partial b}{\partial t} = \frac{\Gamma^3}{12\mu} \frac{\partial}{\partial x} \left\{ \frac{k}{mx} \left[ \frac{\partial b}{\partial x} - \frac{\rho_s \mathcal{L} m}{k T_m} \right] \right\}.$$

This is a modified diffusion equation with spatially varying diffusivity. Now we consider the scaling of this equation. We expect that

$$\frac{b}{x} \sim \frac{\rho_s \mathcal{L} m}{k T_m},$$

on purely dimensional grounds. Also, both sides must balance and therefore

$$\left( \frac{x^3}{b} \right) \left( \frac{b}{t} \right) \sim \frac{k \Gamma^3}{12\mu m}.$$

This gives

$$x \sim \left( \frac{k \Gamma^3 t}{12\mu m} \right)^{\frac{1}{3}} \quad \text{and} \quad b \sim \frac{\rho_s \mathcal{L} m}{k T_m} \left( \frac{k \Gamma^3 t}{12\mu m} \right)^{\frac{1}{3}}.$$

Thus, we can expect a similarity solution of the form

$$b - b_0 = \frac{\rho_s \mathcal{L} m}{k T_m} \left( \frac{k \Gamma^3 t}{12 \mu m} \right)^{\frac{1}{3}} g(\eta) \quad \text{where} \quad \eta = \left( \frac{12 \mu m}{k \Gamma^3 t} \right)^{\frac{1}{3}} x.$$

Inserting these expressions into the nonlinear diffusion equation we have that

$$g'' = \frac{g' - 1}{\eta} + \frac{1}{3} \eta g - \frac{1}{3} \eta^2 g' \quad \text{subject to} \quad g(\eta = 0) = 0 \quad \text{and} \quad g(\eta \rightarrow \infty) = 0.$$

The first boundary condition is because of the hoop stress. Since there is no bending stress, before the ice, there is not deflection. The second boundary condition is that far down the ice there is no change. Note that  $g' = 1$  at  $\eta = 0$ , is forced by the equation. A solution can be found numerically. The tube does not expand indefinitely, but rather stops when the hoop stress balances the thermomolecular pressure. After an infinitely long time, we find a linear deformation profile that arises because of the linear temperature profile.

## 16.2 Particle Migration

In this section we consider the problem of a solid particle in a large block of ice with an applied thermal gradient,  $\nabla T = \underline{G}$ . At a curved solid-liquid interface we must consider the full ClausiusClapeyron relation, given as

$$P_s - P_l = \rho_s \mathcal{L} \frac{T_m - T}{T_m} = P_T + \gamma \nabla \cdot \underline{n}.$$

The term  $P_T$  is the disjoining force and the last term is Gibb-Thomson with the surface energy given by  $\gamma$ . The unit normal vector points from the solid into the liquid. The net disjoining force on the particle can then be computed as

$$\underline{F}_T = - \int_{\mathcal{B}} P_T \underline{n} dS = - \int_{\mathcal{B}} -\gamma (\nabla \cdot \underline{n}) \underline{n} + \rho_s \mathcal{L} \frac{T_m - T}{T_m} \underline{n} dS.$$

The surface  $\mathcal{B}$  is closed. The first integral is a first order isotropic integral that is zero. By the divergence theorem we can simplify the second integral to

$$\underline{F}_T = \frac{\rho_s \mathcal{L}}{T_m} \int_{\mathcal{D}} \nabla T dV.$$

The volume region  $\mathcal{D}$  is the interior, hence the sign change. If the thermal properties of all of the phases are equal and no latent heat is released then  $\underline{G} = \nabla T$  is uniform. This gives

$$\underline{F}_T = \frac{\mathcal{L}}{T_m} \underline{G} m_s = \frac{\mathcal{L}}{T_m} \underline{G} m_I,$$

where  $m_s$  is the mass of the solid and  $m_I$  is the mass of the ice displaced. This is a statement similar to Archimedes principle and is called *thermodynamic buoyancy*. Note that this is independent of the geometry and type of intermolecular force, i.e., Van der Waals etc.

### 16.2.1 Lubrication Analysis

In the frame of reference of the particle we have that

$$\pi (a \sin(\theta))^2 u = (2\pi a \sin(\theta)) q,$$

where

$$q = - \frac{d^3}{12\mu a} \frac{1}{a} \frac{\partial P_l}{\partial \theta}.$$

Combining these two equations we arrive at

$$\frac{\partial P_l}{\partial \theta} = - \frac{6\mu a^2 u}{d^3} \sin(\theta).$$

This means that the geometry matters. Thermodynamic equilibrium gives

$$P_T = \frac{A}{6\pi d^3} = \frac{\rho_s \mathcal{L}}{T_m} [T_m - T_0 - Ga \cos(\theta)] + \frac{2\gamma}{a}.$$

The two terms after  $T_m$  in brackets are the temperature  $T$ , where  $T_0$  is the temperature at the center of the particle. Inserting the expression for  $d^3$  into the pressure derivative we have

$$\frac{\partial P_l}{\partial \theta} = -\frac{36\pi\mu a^2 u}{A} \left[ \frac{\rho_s \mathcal{L}}{T_m} [T_m - T_0 - Ga \cos(\theta)] + \frac{2\gamma}{a} \right] \sin(\theta).$$

Integrating this expression yields

$$P_l = P_0 - \frac{36\pi\mu a^2 u}{A} \left[ \frac{\rho_s \mathcal{L}}{T_m} \left[ T_m - T_0 - \frac{1}{2} Ga \cos(\theta) \right] + \frac{2\gamma}{a} \right] \cos(\theta).$$

The  $1/2$  appears in front of the  $G$  term because of the integration. We can then compute the viscous force  $F_\mu$ , as

$$\underline{F}_\mu = - \int_{\mathcal{B}} P_l \underline{n} \, dS = -\frac{4}{3} \pi a^3 \frac{\mu \underline{u}}{\Pi}.$$

The coefficient  $\Pi$  is an effective *permeability* and is given as

$$\Pi = \frac{A}{36\pi a} \left[ \frac{\rho_s \mathcal{L}}{T_m} (T_m - T_0) + \frac{2\gamma}{a} \right]^{-1}.$$

In the absence of gravity we have that

$$\underline{F}_T + \underline{F}_\mu = 0.$$

This gives that the particle migrates in the direction of temperature gradient with a velocity

$$\boxed{\underline{u} = \frac{\rho_s \mathcal{L} \Pi}{\mu T_m} \underline{G}.}$$

This is problematic for the dating of particles in ice cores.

## References

- G.K. Batchelor, H.K. Moffatt, and M.G. Worster, editors. *Perspectives in Fluid Dynamics*. Cambridge University Press, 2000.
- E. J. Hinch. *Perturbation Methods*. Cambridge University Press, 1991.
- H. E. Huppert and M. G. Worster. Dynamic solidification of a binary melt. *Nat.*, 314:703–707, 1985.
- A. Umantsev. Motion of a plane front during crystallization. *Sov. Phys. Crystallogr.*, 30:87–91, 1985.
- M. G. Worster. Solidification of an alloy from a cooled boundary. *J. Fluid Mech.*, 167:481–501, 1986.